Confinement and Deconfinement in Gauge Theories

by

Kieran Holland

Submitted to the Department of Physics
in partial fulfillment of the requirements for the degree of

Doctor of Philosophy

at the

MASSACHUSETTS INSTITUTE OF TECHNOLOGY

June 1999

Author .....
Department of Physics
June 4th, 1999

Certified by .....
Uwe-Jens Wiese
Associate Professor
Thesis Supervisor

Accepted by .....
Thomas J. Greytak
Associate Department Head for Education

Confinement and Deconfinement in Gauge Theories

by

Kieran Holland

Submitted to the Department of Physics
on June 4th, 1999, in partial fulfillment of the
requirements for the degree of
Doctor of Philosophy

Abstract

In this thesis, we examine properties of the confined and deconfined phases of non-Abelian gauge theories. In one part of the thesis, we examine a String Theory prediction made for Supersymmetric Yang-Mills theory. The prediction is that a QCD string emanating from a quark and carrying color flux can end on a domain wall which has no color charge. Using effective field theoretic methods, we explain how the domain wall carries the color flux of the QCD string to spatial infinity. We use this explanation to predict the phase structure of Supersymmetric Yang-Mills theory. We also examine universal critical phenomena associated with these domain walls. In the rest of the thesis, we show analytically how static test quarks can be confined, even in the deconfined bulk phase. We observe this unusual confinement numerically in an effective field theory for the gauge theory using highly efficient cluster techniques. This is also a new method to determine the energy cost of domain walls separating bulk phases.

Thesis Supervisor: Uwe-Jens Wiese
Title: Associate Professor

Acknowledgments

First and foremost, I would like to thank my thesis supervisor Uwe-Jens Wiese. It has been a pleasure and a privilege to work with him and I cannot thank him nearly enough for all his direction, advice and assistance in all of the projects on which we have worked together. He has been a superb mentor and I hope the highest compliment that I can pay him is that, if I had the chance to start over and choose a new supervisor, I would gladly choose him again.

I would like to thank Antonio Campos, with whom we had a most fruitful and enjoyable collaboration and learned quite a lot along the way, and Ben Scarlet, with whom we worked so diligently on a problem that was damned if we could solve it. I wish to thank the following people for their various contributions in the work I've done, whether they were large or small: Sergei Bashinsky, Richard Brower, Victor Chudnovsky, Jürgen Cox, Shailesh Chandrasekharan, Dong Chen, Eddie Farhi, Jeffrey Goldstone, Andrew Pochinsky, Antonios Tsapalis.

I would like to thank the directors, staff and members of the Center for Theoretical Physics, without whose support, financial and otherwise, this work would not have been carried out. I also wish to acknowledge the receipt of partial support from the U.S. Department of Energy (D.O.E.) under cooperative research agreement DE-FC02-94ER40818.

I would like to thank the members of my thesis committee, Prof. Jeffrey Goldstone and Prof. Patrick Lee.

I cannot forget to mention some fellow '95 CTP recruits: Noah Graham, Oliver DeWolfe and Tamás Hauer. Thank you for all that I've learned from our many and varied conversations, if I forget the physics, I hope to remember the baseball.

There are many I wish to include, for brevity's and modesty's sake, first names only: Allen, Jeff, Jim, the Atomic Balldrivers, the Tang Hall/Chemistry/European Club soccer team, the swimming coaches, Frau Crocker, the students of 8.01X, the MIT Community Players and many others. It's all been part of the certainly unique MIT experience.

I have to thank my housemates of the last three years, Dan, David and Winthrop. I'm sorry that the 11 Simpson Ave. pack is breaking up, it's been a pleasure to live with you guys. The very best of luck to you and I hope we can all keep in touch.

To all my friends in so many scattered places, I promise I will e-mail you more often.

To my family, for all their support, I hope they continue to be proud of what I've done and happy that I've chosen it.

Finally to Elke, you may never read this thesis, but at least I hope you understand why it means as much to me as you do.

Contents

Chapter 1

Introduction

1.1 Thesis Summary

There is overwhelming evidence that Quantum Chromodynamics (QCD) is the fundamental theory underlying the strong interaction of hadrons. QCD is the non-Abelian gauge theory with a local $SU(3)$ symmetry. It describes the interaction of particles which carry color charge. In the theory, there are fermions known as quarks which interact via gluons, the color-charged gauge bosons. Although the particles of the underlying theory carry color charge, this charge is not carried by the hadrons which interact by the strong nuclear force. In order for QCD to be the correct fundamental description of the strong interaction, there must be some reason why the color charge is not directly observable. This is explained by a mechanism known as confinement, in which quarks and gluons dynamically combine in a fashion to produce physically observable particles which are color-neutral.

We first look at pure Yang-Mills theory i.e. QCD without dynamical quarks. We consider a single static test quark which carries color charge and from which color flux lines emanate. In electromagnetism, the flux lines coming out of an electrically charged object spread out in all directions and produce a $1/R$ potential between two static electrical charges separated by a distance R. However, unlike photons, gluons carry color charge and interact with one another. The color flux lines are attracted to each other and bunch together into a fluctuating tube. Viewed at larger scales,

this tube looks like a fluctuating string and is known as the QCD string. This string has an energy cost proportional to its length and the energy cost per unit length is the string tension σ. The QCD string emanating from the quark ends on an anti-quark which has the opposite color charge. The potential between a static quark and anti-quark separated by a distance R is

$$V(R) = \sigma R + O(1/R). \tag{1.1}$$

The linear term is due to the energy cost of the QCD string connecting the quark and anti-quark and the $1/R$ term is due to fluctuations of the string [1]. If we want to observe color charge by isolating a single quark, we need to separate the quark from all other quarks, forcing $R \to \infty$. But this would cost an infinite amount of energy and is not possible. The formation of the QCD string means physical states with a finite energy cost must be color-neutral. This is the confinement mechanism which prevents us from observing an isolated quark with color charge. If we return to full QCD with dynamical quarks, we cannot make the QCD string arbitrarily long. If we separate a quark-anti-quark pair sufficiently far from each other, it is energetically favorable for the string to break and to produce two color-neutral quark-anti-quark pairs.

The confinement mechanism is due to the formation of the QCD string which occurs because the gluons, which carry color charge, interact with each other. Confinement is a very important property of non-Abelian gauge theories and it explains why it is possible for QCD to be the correct microscopic description of the strong interaction. However, there are phases of QCD where confinement is not expected to occur. Due to asymptotic freedom [2], the QCD coupling becomes small at very high energy scales and there is evidence that quarks and anti-quarks are no longer connected by QCD strings. Instead, there is a quark-gluon plasma, where a quark-anti-quark pair has a Debye potential

$$V(R) = \frac{\exp(-R/R_D)}{R}, \tag{1.2}$$

where R_D is the Debye or screening length. In this regime, where quarks are said to be deconfined, it does not cost an infinite amount of energy to isolate a quark. The color charge is no longer confined, but is screened by the plasma. This is the deconfined phase of the theory. We will examine several interesting phenomena associated with confinement and deconfinement in non-Abelian gauge theories.

In Chapter 2, we examine Supersymmetric (SUSY) Yang-Mills theory which is very similar to QCD. It contains gluons and fermions known as gluinos. There are differences between these gluinos and the quarks of QCD. Despite these differences, there are strong similarities between the theories. It is expected that there are confined and deconfined phases in SUSY Yang-Mills theory, as in QCD. These properties are thought to be due to the non-Abelian nature of the gauge group and are not affected by other symmetries a theory may have. Also, both theories have global symmetries which are related to the fermions being in purely left- or right-handed states. These symmetries may be spontaneously broken in the quantized theory. This handedness or chiral symmetry is another central feature of QCD. We examine a claim made by Witten using Matrix-Theory techniques in String Theory. He describes a phenomenon in SUSY gauge theory, in which a QCD string emanating from a static test quark does not end on an anti-quark, but on a color-neutral domain wall which separates distinct bulk phases. We look at this claim using effective field theory and find a simpler explanation of how the phenomenon occurs [3]. We use this explanation to predict the phase structure of SUSY Yang-Mills theory. We also examine some very interesting critical properties of the domain walls, for example the splitting of one wall into two. We show that this behavior belongs to well-known universality classes.

In Chapter 3, we look at the deconfinement phase transition of Yang-Mills theory. This phase transition has an order parameter, whose finite volume behavior we examine. From the order parameter, we extract the free energy of a static test quark. We find analytically that, even deep in the deconfined phase of the theory, a static test quark can be confined [4]. The phenomenon is due to the deconfined phase having multiple degenerate bulk phases. In cylindrical volumes, the distinct deconfined bulk

phases line up into domains, separated by domain walls. This unusual confinement links the free energy of a single static quark to the energy cost of these domain walls. This is evidence that the domain walls are not artefacts which only exist in Euclidean space-time but that they are actual physical objects in Minkowski time. We also find analytically the finite volume dependence of the quark free energy close to the phase transition. Our analytical calculations present a new method for extracting the energy cost of the domain walls from muerical simulations performed at finite volume.

In Chapter 4, we examine a spin model which is an effective theory for the Yang-Mills deconfinement phase transition [5]. In this effective theory, we successfully observe numerically the analog of unusual confinement in the deconfined phase of Yang-Mills theory, as was predicted analytically in Chapter 3. We build a cluster algorithm which allows us to efficiently measure exponentially small numerical signals, which would otherwise be unobservable. We also exploit the finite volume dependence of the quark free energy to extract the energy cost of domain walls far away from and close to the phase transition.

In the remainder of this Chapter, we describe some of the essential features of Yang-Mills theory, QCD and Supersymmetric Yang-Mills theory.

1.2 Features of Yang-Mills theory

1.2.1 Gauge symmetry

Pure gauge or Yang-Mills theory describes the interaction of dynamical gauge bosons. In a non-Abelian gauge theory, the gauge bosons interact non-trivially to produce some of the features of full QCD with dynamical quarks. For Yang-Mills theory with an $SU(N)$ gauge symmetry, the gauge fields are $A_\mu(\vec{x},t) = ieA^a_\mu(\vec{x},t)\lambda_a, a = 1,...,N^2-1$, where λ_a are the generators of the group $SU(N)$ and e is the coupling of the theory. The gauge fields are also known as gluons. In Euclidean space-time,

the action is

$$S[A_\mu] = \int dt d^3x \frac{1}{2e^2} \mathrm{Tr} F_{\mu\nu}(x) F_{\mu\nu}(x), \tag{1.3}$$

where $F_{\mu\nu} = \partial_\mu A_\nu - \partial_\nu A_\mu + [A_\mu, A_\nu]$ is the field strength. The field strength is a matrix and so in the action we take the trace of the gauge field kinetic term. Because of the commutator term in the field strength, the action contains terms with three and four gauge fields. These terms describe three- and four-gluon interaction vertices. This basic property distinguishes Yang-Mills theory from electromagnetism, where photons do not interact with one another, and makes the non-Abelian gauge theory non-trivial. The gauge fields transform under gauge transformations as

$$A'_\mu(x) = g(x)(A_\mu(x) + \partial_\mu) g^+(x) \qquad \longrightarrow \qquad F'_{\mu\nu}(x) = g(x) F_{\mu\nu}(x) g^+(x). \tag{1.4}$$

The action contains the trace of the gluon kinetic term and, as the trace is cyclic, the action is invariant under gauge transformations.

We described the mechanism by which quarks carrying color charge are confined due to the formation of a QCD string carrying the color flux. There are no quarks in Yang-Mills theory, only gluons, which also carry color charge. In the confined phase, we should not be able to observe this color charge. In fact, the gluons interact dynamically so that the lowest energy state above the vacuum is a colorless massive particle, the glueball. The fact that this state is massive is sometimes described by saying that the theory has a mass gap.

1.2.2 Temperature of field theory

Given a field theory in Euclidean space-time, we can construct the Hamilton operator $\mathcal{H}$ of this theory. This operator describes how the system propogates in the Euclidean time direction. The partition function of the quantum theory at some non-zero temperature T is

$$Z = \mathrm{Tr} \exp(-\beta \mathcal{H}), \tag{1.5}$$

where $\beta = 1/T$ is the inverse temperature and we take the trace over all quantum states. The operator $\exp(-\beta\mathcal{H})$ propogates an initial state of the system forward in the time direction by an amount β to some final state. The trace of the operator is the sum of the diagonal elements, so only if the initial and final states are the same is a contribution made to the partition function. If the system is periodic in the time direction with time extent β, this time extent is the inverse temperature.

If we choose a basis of fields ϕ_k for the states, the partition function is the functional integral

$$Z = \int \prod_k [D\phi_k] \exp(-S_E[\phi_k]). \tag{1.6}$$

S_E is the Euclidean action of the theory and the measure of integration is contained in $[D\phi_k]$. The inverse temperature β is now contained as the time extent in the periodic time direction in the Euclidean action. When we describe a field theory as being at high or low temperature, we mean the Euclidean time extent is small or large.

1.2.3 Confinement at non-zero temperature

For Yang-Mills theory, the Euclidean form of the action at non-zero temperature is

$$S_E[A_\mu] = \int_0^\beta dt \int d^3x \frac{1}{2e^2} \mathrm{Tr} F_{\mu\nu}(x) F_{\mu\nu}(x). \tag{1.7}$$

The gauge field is periodic in the time direction, $A_\mu(\vec{x}, t+\beta) = A_\mu(\vec{x}, t)$, as are the gauge transformations. We can learn about whether or not confinement of static test quarks occurs in this theory from a field known as the Wilson line or Polyakov loop [6],

$$\Phi(\vec{x}) = \mathrm{Tr}[\mathcal{P} \exp(\int_0^\beta dt A_4(\vec{x}, t))] \in \mathbf{C}. \tag{1.8}$$

This complex field is a trace over the path-ordered exponential of the integral of the Euclidean time component of the gauge field along the time direction. The Polyakov loop measures the response of the dynamical gluons to a static test quark which propagates forward in Euclidean time sitting at position $\vec{x}$. Quantitatively, the free energy F of the static test quark in this background is given by the real part of the

Polyakov loop expectation value $\mathrm{Re}\langle\Phi\rangle = \exp(-\beta F)$. If a quark is confined, this means that as we try to isolate the quark by pulling it arbitrarily far away from other quarks, its free energy becomes infinite. If $F \to \infty$, then $\langle\Phi\rangle \to 0$. However, if a quark is deconfined, then the free energy does not diverge as we isolate it from all other quarks and $\langle\Phi\rangle \not\to 0$. Thus, measuring the expectation value of the Polyakov loop tells us which phase of the theory we are in.

As well as the continuous gauge symmetry, the Yang-Mills action at non-zero temperature also has a discrete global symmetry. If the gauge group is $SU(N)$ and if the gauge transformations are not quite periodic in the time direction, but are instead twisted

$$g(\vec{x}, t+\beta) = g(\vec{x}, t)z, z \in \mathbf{Z}(N) = \{\exp(2\pi i n/N), n = 1, ..., N\}, \tag{1.9}$$

the action is still invariant. The gauge transformation of the field strength is $F'_{\mu\nu} = gF_{\mu\nu}g^+$, so the twisted gauge group elements g and g^+ would contain z and z^* respectively, where $*$ denotes complex conjugate. As $zz^* = 1$, the gauge transformation is unchanged and the cyclicity of the trace means the action is invariant, as before. This global symmetry is known as the $\mathbf{Z}(N)_c$ center symmetry of the theory. However, the Polyakov loop transforms non-trivially if the gauge group elements are twisted. It changes by

$$\begin{aligned} \Phi'(\vec{x}) &= \mathrm{Tr}[\mathcal{P}\exp(\int_0^\beta dt A'_4(\vec{x}, t))] \\ &= \mathrm{Tr}[g(\vec{x}, 0)\mathcal{P}\exp(\int_0^\beta dt A_4(\vec{x}, t))g^+(\vec{x}, 0)z^*] = \Phi(\vec{x})z^*. \end{aligned} \tag{1.10}$$

Although the action has the global symmetry, this may be spontaneously broken in the quantized theory. If $\langle\Phi\rangle = 0$, then the center symmetry is unbroken, as zero times z^* is still zero. If $\langle\Phi\rangle \neq 0$, then the center symmetry is broken. The Polyakov loop is the order parameter for this symmetry. An order paramater is a quantity which vanishes in one phase of a theory and is non-zero in another. If $\langle\Phi\rangle = 0$, the free energy of a static quark diverges, meaning that it is confined. If $\langle\Phi\rangle \neq 0$, the

static quark free energy does not diverge and the quark is deconfined. If the center symmetry is intact, we are in the confined phase of the theory, if the symmetry is broken, we are in the deconfined phase [7].

Previous work has shown that the center symmetry is spontaneously broken at high temperatures in Yang-Mills theory. Because the discrete $\mathbf{Z}(N)_c$ symmetry is broken, there are N distinct degenerate deconfined bulk phases. These bulk phases are distinguished from one another by their values of the Polyakov loop expectation value $\langle\Phi\rangle = \Phi^{(n)} = \Phi_0 \exp(2\pi i n/N), n \in \{1, ..., N\}$, which are related to one another by $\mathbf{Z}(N)_c$ rotations. As one goes from low to high temperature, we encounter a phase transition as we cross from the confined to the deconfined phase. The order of this phase transition is dependent on the gauge group. A conjecture was put forward that the effective theory describing this deconfinement phase transition in a $(d+1)$-dimensional Yang-Mills theory is a d-dimensional spin model which contains the center symmetry. The belief is that the important degree of freedom is the Polyakov loop. For example, for 4-dimensional $SU(2)$ Yang-Mills theory, the deconfinement phase transition should have the properties of the ordering phase transition in a 3-dimensional spin model with $\mathbf{Z}(2)$ symmetry. This is the Ising model with spins ± 1, which has a second order phase transition. If the gauge group is $SU(3)$, the spin model is the 3-state Potts model, which is the generalization of the Ising model to complex spins $\exp(2\pi i n/3), n \in \{1, 2, 3\}$ and which has a $\mathbf{Z}(3)$ symmetry. Numerical studies have shown that this spin model has a first order phase transition [8]. It has been shown by numerical work that this pattern is indeed observed. $SU(2)$ pure gauge theory undergoes a second order phase transition, with an infinite correlation length and the universal critical behavior in the bulk is that of the Ising model [9]. On the other hand, $SU(3)$ pure gauge theory has a first order phase transition, with a finite correlation length and no universal critical bulk behavior [10].

1.2.4 Confinement at zero temperature

Pure Yang-Mills theory at non-zero temperature has the global $\mathbf{Z}(3)_c$ center symmetry, associated with the gauge transformations being twisted in the periodic time

direction. The Polyakov loop is the order parameter which tells us if this symmetry is intact or not. If it is intact, i.e. $\langle\Phi\rangle = 0$, we are in the confined phase and if it is spontaneously broken, $\langle\Phi\rangle \neq 0$, we are in the deconfined phase. If we go to zero temperature, the time extent becomes infinite. We can no longer construct the Polyakov loop by integrating over the time direction and the center symmetry is absent, as we cannot twist gauge transformations in the time direction. There is no symmetry from whose order parameter we can detect confinement.

We can see whether or not confinement occurs at zero temperature from the Wilson loop

$$W(C) = \mathrm{Tr}[\mathcal{P}\exp(\oint_C dx_\mu A_\mu)], \tag{1.11}$$

which is the trace of the path-ordered exponential of the integral of the gluons around a closed loop C. We can choose the loop to be rectangular, with extent T in the Euclidean time direction and extent R in the spatial direction. The Wilson loop then represents a static quark and anti-quark which are created at some instant a distance R apart from one another. The quark and anti-quark propogate forward for a time T at a constant spatial separation and then they are simultaneously annihilated. Then the expectation value of the Wilson loop is

$$\langle W(R,T)\rangle = \exp(-V(R)T), \tag{1.12}$$

where $V(R)$ is the potential between the quark and the anti-quark. If the dominant contribution to the Wilson loop expectation value depends on the area of the closed loop $\langle W(R,T)\rangle = \exp(-\sigma A), A = RT$, then the potential is $V(R) \approx \sigma R$. This linear potential is due to a QCD string connecting the quark and anti-quark and so we see that we are in the confined phase. However, if the dominant contribution to $\langle W(R,T)\rangle$ depends on the perimeter of the loop, then the potential V does not diverge as the separation R is made large and we see that we are in the deconfined phase.

At non-zero temperature, we can also construct Wilson loops whose time extent is less than β. If the gauge transformations are twisted by z, the Wilson loop contains

both factors z and z^* and is unchanged — it is not sensitive to the center symmetry. A non-zero value for $\langle W \rangle$ does not break the center symmetry, so the Wilson loop is not an order parameter.

1.2.5 Confinement phase transition in Early Universe

There are very interesting cosmological questions related to the deconfinement phase transition [11]. After the Big Bang, when the Universe was very hot, it is believed that quarks and gluons lived in a plasma. As the Universe expanded and cooled, at some point this quark-gluon plasma changed into the hadronic world of protons, neutrons and so on. It is of interest to know whether this change was a phase transition, if so, then what was the order of the QCD phase transition and are there any relics of it left in the Universe?

If we ignore dynamical quarks and look only at pure Yang-Mills theory, we can describe the behavior of the phase transition. This hypothetical Universe, which has been simulated on the lattice, contains only gluons. The QCD gauge group is $SU(3)$ and so, in the early stages of the Universe when the temperature was very high, we would have been in the deconfined phase of the theory, with three distinct deconfined bulk phases. The Universe would have been filled with deconfined domains, whose sizes were of the order of the bulk correlation length and which were separated by domain walls. These domain walls have an energy cost proportional to their area. At the first order phase transition, the three deconfined phases coexist with one confined phase. As the Universe cooled and approached the critical temperature, one would expect that tiny bubbles of confined phase would be formed in the bulk by supercooling and that these bubbles would grow macroscopic in size. If bubble nucleation took place throughout the Universe, there would be no large scale structure left behind [12].

However, the network of deconfined domain walls may also have affected the formation of the hadronic phase. It has been shown for $SU(3)$ Yang-Mills theory that, as we approach the phase transition, a deconfined-deconfined domain wall between two distinct deconfined phases splits into two parallel domain walls, sandwiching a thin

film of confined phase between them. As we approach the critical temperature, the thin film expands and pushes the two deconfined-confined domain walls apart. This phenomenon of a domain wall splitting into two is complete wetting and occurs frequently in particle and condensed matter physics [13]. It is a universal phenomenon whose behavior is governed by critical indices of a well-defined universality class. Complete wetting suggests that, in a hypothetical early Universe which contains only gluons, the confined phase was formed by the splitting of the network of deconfined-deconfined domain walls. This method of creating the hadronic phase might leave some large scale relic of the domain wall network in this hypothetical Universe. However, the real Universe also contains quarks, which make the domain walls unstable, as the degeneracy of the three deconfined phases is broken and one phase becomes the absolute minimum. It is expected that the domain walls would have vanished before the QCD phase transition occured and so they should have left no trace behind.

1.3 Features of QCD

1.3.1 Gauge symmetry

In general, we can have a non-Abelian gauge theory with the gauge group $SU(N)$ and with N_f flavors of color-charged quarks $\Psi_{fc}(x), f \in \{1, ..., N_f\}, c \in \{1, ..., N\}$. As in the Yang-Mills theory, there are also gluons $A^a_\mu(x), a \in \{1, ..., N^2 - 1\}$. QCD is the specific theory with N_f flavors of quarks in the fundamental representation of the gauge group $SU(3)$. The Euclidean QCD action is

$$S_{QCD}[\Psi, \bar{\Psi}, A_\mu] = \int dt d^3x \{ \sum_f \bar{\Psi}_f(x)(\gamma_\mu(\partial_\mu + A_\mu(x)) + m_f)\Psi_f(x) + \frac{1}{2e^2}\mathrm{Tr}F_{\mu\nu}(x)F_{\mu\nu}(x)\}. \tag{1.13}$$

The action is invariant under local color-space rotations of the quarks and gluons

$$\begin{aligned} \Psi_{fc'}(x) = \sum_c g_{c'c}(x)\Psi_{fc}(x) \qquad & \text{i.e.} \qquad \Psi_f(x) = g(x)\Psi_f(x) \\ A'_\mu(x) = g(x)(A_\mu(x) + \partial_\mu)g^+(x) \quad \rightarrow \quad & F'_{\mu\nu}(x) = g(x)F_{\mu\nu}g^+(x), \end{aligned} \tag{1.14}$$

where g is an element of the group $SU(3)$. The same gauge transformation is applied to all quark flavors. If the quark flavors did not mix with each other, we could apply different gauge transformations to each flavor. However, the weak interaction does mix the quark flavors and so they cannot be transformed independently.

1.3.2 Confinement

In Yang-Mills theory at non-zero temperature, we can detect confinement by seeing whether the $\mathbf{Z}(3)_c$ center symmetry is intact or spontaneously broken. In Yang-Mills theory at zero temperature, we are in the confined phase if the Wilson loop has an area dependence, which means the quark-anti-quark potential is linear in the separation.

In QCD at non-zero temperature, the center symmetry is explicitly broken by the quarks, as they transfrom under the fundamental representation of the gauge group. We cannot use the center symmetry to detect confinement. At zero temperature, the Wilson loop need no longer have an area dependence in the confined phase, as the surface of the loop can be eaten by small holes created by dynamical quark-anti-quark loops. In the confined phase, the potential between a quark and an anti-quark is linear at small distances, then reaches a plateau as the QCD string is broken. To detect confinement in full QCD, one must show that the physical states are colorless.

1.3.3 Chiral symmetry

QCD does not have the discrete $\mathbf{Z}(3)_c$ center symmetry of Yang-Mills theory. However, if some or all of the quark flavors are massless, QCD does have a continuous global symmetry. We can decompose a fermion into left- and right-handed components

$$\begin{aligned}
\Psi &= \frac{(1-\gamma_5)}{2}\Psi + \frac{(1+\gamma_5)}{2}\Psi = \Psi_L + \Psi_R, \\
\Psi^+ &= \Psi^+\frac{(1-\gamma_5)}{2} + \Psi^+\frac{(1+\gamma_5)}{2} = \Psi_L^+ + \Psi_R^+, \\
\bar{\Psi} &= \Psi^+\gamma_0 = \bar{\Psi}\frac{(1+\gamma_5)}{2} + \bar{\Psi}\frac{(1-\gamma_5)}{2} = \bar{\Psi}_L + \bar{\Psi}_R, \\
\gamma_5 &= \gamma_5^+, \qquad \gamma_5^2 = \gamma_5, \qquad \{\gamma_5, \gamma_\mu\} = 0, \quad \mu = 1, ..., 4.
\end{aligned} \tag{1.15}$$

The only term in the Lagrangian which mixes left- and right-handed components is the mass term

$$m_f \bar{\Psi}_f \Psi_f = m_f(\bar{\Psi}_{fL}\Psi_{fR} + \bar{\Psi}_{fR}\Psi_{fL}). \tag{1.16}$$

If we consider the case where the N_f quark flavors are massless, then we can make global rotations in flavor-space of the left- and right-handed components of these massless quark flavors independently, i.e.

$$\begin{aligned} U(N_f)_L: &\quad \Psi'_L = U_L\Psi_L, \qquad \Psi'_R = \Psi_R, \qquad U_L \in U(N_f)_L \\ U(N_f)_R: &\quad \Psi'_R = U_R\Psi_R, \qquad \Psi'_L = \Psi_L, \qquad U_R \in U(N_f)_R \end{aligned} \tag{1.17}$$

and the Lagrangian is unchanged. At the level of the Lagrangian, the symmetry group is

$$U(N_f)_L \otimes U(N_f)_R = SU(N_f)_L \otimes SU(N_f)_R \otimes U(1)_B \otimes U(1)_A, \tag{1.18}$$

where $U(1)_B$ is associated with baryon number and $U(1)_A$ is the axial symmetry. In the fully quantized theory, the $U(1)_A$ axial symmetry is broken anomalously, which we will discuss later. The global symmetry group is reduced to $SU(N_f)_L \otimes SU(N_f)_R \otimes U(1)_B$, of which $SU(N_f)_L \otimes SU(N_f)_R$ is known as chiral symmetry. Although the classical Lagrangian may by chirally symmetric, it is possible for the symmetry to be spontaneously broken in the quantized theory. In the quantum theory, it is possible for all the massless quark flavors to obtain a non-zero expectation value for the quark-anti-quark bilinear, i.e. $\langle\bar{\Psi}\Psi\rangle \neq 0$. Under independent left- and right-handed transformations, the bilinear transforms as

$$\langle\bar{\Psi}\Psi\rangle = \langle\bar{\Psi}_L\Psi_R\rangle + \langle\bar{\Psi}_R\Psi_L\rangle \longrightarrow \langle\bar{\Psi}_L U_L^+ U_R\Psi_R\rangle + \langle\bar{\Psi}_R U_R^+ U_L\Psi_L\rangle. \tag{1.19}$$

The bilinear is invariant only if $U_L = U_R$, i.e. left- and right-handed rotations are the same. This reduces the global symmetry

$$SU(N_f)_L \otimes SU(N_f)_R \longrightarrow SU(N_f)_{L=R}, \tag{1.20}$$

as we can no longer make independent flavor rotations of the left- and right-handed components of the massless quarks. The chiral symmetry is broken by the quark-anti-quark bilinear, which is the quark condensate.

1.3.4 Approximate chiral symmetry in Nature

In QCD, none of the quark flavors are massless. However, in comparison to the energy scale of QCD, $\Lambda_{QCD} \approx 200$ MeV, the up and down quarks both have a very small mass, less than 10 MeV. Whether the strange quark, with a mass of roughly 100 MeV is light or not is debatable. These light quark flavors give us an approximate chiral symmetry. The breaking of an exact continuous global symmetry generates Goldstone bosons [14]. If the chiral symmetry breaking pattern is $SU(N_f)_L \otimes SU(N_f)_R \longrightarrow SU(N_f)_{L=R}$, we expect that $N_f^2 - 1$ Goldstone bosons are generated. Breaking an approximate chiral symmetry, we expect to generate pseudo-Goldstone bosons, particles which are light and would be massless if the symmetry was exact.

Taking the up and down quark as massless, we identify the three pions π^+, π^- and π^0 as the Goldstone bosons. If we include the strange quark as massless, then the four kaons $K^+, K^-, K^0, \bar{K}^0$ and the eta particle η are also the products of broken chiral symmetry. This correct identification of the lightest hadrons means that QCD has an approximate chiral symmetry. If the chiral symmetry were exact, then the breaking of this global symmetry would be a phase transition. The order of this phase transition is dependent on the number of massless quark flavors. Studies of models which have the same symmetries show that for two massless flavors, the phase transition is second order, while for three massless flavors, the phase transition is first order. As discussed for Yang-Mills theory, the order of the phase transition influences the creation of the

hadronic phase in the early Universe. It is unclear whether the strange quark is approximately massless in this context and if the creation of hadronic matter is a first order phase transition or at best a crossover for light quarks [15].

1.3.5 Confinement and chiral symmetry breaking

Going from low to high temperature, pure gauge theory has a deconfining phase transition where the center symmetry is broken. In QCD with massless quarks, going from low to high T, there is a phase transition where chiral symmetry is restored. Although QCD does not have the center symmetry, the confining behavior seems to change in the same temperature region as chiral symmetry restoration [16]. Quantities such as the energy and entropy density and the pressure increase rapidly in this region, as a result of the release of the color degrees of freedom via deconfinement. The Polyakov loop value also increases considerably in this temperature range, while other quantities, the Polyakov loop and quark condensate susceptibilities, have pronounced peaks near the same temperature. Although there is no symmetry associated with confinement in QCD, there is evidence that there is an onset of deconfinement just as chiral symmetry is being restored.

It had been speculated that deconfinement and chiral symmetry restoration occur at two distinct temperatures, with deconfinement taking place at the lower temperature [17]. The evidence from numerical studies is that these phenomena coincide. We are not able to use symmetry arguments in QCD to investigate this. We show in Chapter 2 that we can make a connection between deconfinement and chiral symmetry restoration in supersymmetric gauge theory.

1.4 Features of Supersymmetric gauge theory

1.4.1 Possible symmetries

It has been shown that, under some very general assumptions, there are very few types of symmetries that are compatible with quantum field theory [18]. There are sym-

metries associated with space-time transformations, i.e. Lorentz invariance. There are internal symmetries, e.g. rotations of quarks in color-space. The third type is symmetries of transformations between bosons and fermions. Such symmetries are supersymmetries and as yet are the only ones not to have been observed in Nature. There are very interesting properties associated with supersymmetric theories which allow us to explore features in common with non-supersymmetric gauge theories.

The simplest supersymmetric non-Abelian gauge theory we can look at is $\mathcal{N} = 1$ Supersymmetric (SUSY) Yang-Mills theory with the gauge group $SU(N)$, whose Lagrangian we write explicitly as

$$\mathcal{L} = -\frac{1}{4e^2} F^a_{\mu\nu}(x) F^{\mu\nu}_a(x) + \frac{1}{e^2} i \bar{\Psi}_a(x) \gamma^\mu D_\mu \Psi^a(x). \tag{1.21}$$

The field strength matrix is $F_{\mu\nu} = F^a_{\mu\nu} \lambda_a$, λ_a being the generators of the gauge group. The fermions transform under the adjoint representation of the gauge group, so the covariant derivative is

$$D_\mu \Psi^a = \partial_\mu \Psi^a + g f^{abc} A^b_\mu \Psi^c, \tag{1.22}$$

where f^{abc} are the structure constants of the gauge group, defined by $[\lambda_a, \lambda_b] = i f^{abc} \lambda_c$. By $\mathcal{N} = 1$ supersymmetry, we mean that there is only one boson-fermion symmetry, one conserved current and one charge. As in non-supersymmetric Yang-Mills theory, there are gluons $A^a_\mu, a \in \{1, ..., N^2 - 1\}$, which are bosons. In addition, the gluons have an equal number of fermionic partners, the gluinos Ψ^a, which are Majorana fermions. A Majorana particle is one which cannot be distinguished from its antiparticle, i.e. $\Psi = C \bar{\Psi}^T$, where C denotes charge-conjugation and T means the transpose. As the gluinos transform under the adjoint representation, just like the gluons, this distinguishes them from quarks, which transform under the fundamental representation. There is only one flavor of massless gluino, which is necessary for them to be the supersymmetric partners of the massless gluons. The supersymmetry of the theory is that we can make a rotation of the gluons and gluinos into one another which leaves the action invariant.

SUSY Yang-Mills theory is very closely related to QCD. It is asymptotically free

and at low temperatures is expected to have confinement and chiral symmetry breaking. At high temperatures, chiral symmetry is restored and confinement is lost. As in QCD, there seems to be some connection between confinement and chiral symmetry breaking. These are thought to be properties connected to the theory being non-Abelian and are not affected by any additional symmetry constraints. Much work has shown that non-perturbative results can be extracted from the theory by assuming that supersymmetry is unbroken and that only analytic effective potentials are generated by integrating out high energy degrees of freedom [19]. This work shows, for example, that the chiral symmetry of SUSY pure gauge theory is broken non-perturbatively. Because there is only one flavor of massless gluino, we do not have the continuous chiral symmetry of QCD, where we can rotate massless quark flavors into one another. However, SUSY Yang-Mills theory does have an exact discrete chiral symmetry, which we discuss below.

1.4.2 Axial anomaly and discrete chiral symmetry

The $U(1)_A$ axial symmetry is completely broken in QCD by the quantum anomaly [20]. This classical symmetry acts only on the N_f flavors of massless quarks

$$U(1)_A : \Psi' = \exp(i\theta\gamma_5)\Psi, \bar{\Psi}' = \bar{\Psi}\exp(i\theta\gamma_5), \tag{1.23}$$

which leaves the action invariant. However, the quantum theory is generated by the functional integral over all field configurations.

$$Z = \int [D\Psi][D\bar{\Psi}][DA_\mu] \exp(-S_{QCD}[\Psi, \bar{\Psi}, A_\mu]). \tag{1.24}$$

The integration measure is affected by the axial transformation and the functional integral becomes

$$Z' = \int [D\Psi][D\bar{\Psi}][DA_\mu] \exp[-S_{QCD} + \frac{i\theta N_f e^2}{32\pi^2} \int d^4x \mathrm{Tr} F_{\mu\nu}(x)\tilde{F}_{\mu\nu}(x)], \tag{1.25}$$

where the Euclidean dual field strength is defined by $\tilde{F}_{\mu\nu} = \epsilon_{\mu\nu\alpha\beta}F_{\alpha\beta}$, where $\epsilon_{1234} = 1$ and $\epsilon_{\mu\nu\alpha\beta}$ is totally antisymmetric in its indices. The extra term generated by the transformation is the quantum anomaly and is the topological charge. This term is gauge invariant and in fact we could have included it in the original QCD Lagrangian with some coefficient θ_0. The axial transformation would correspond to the shift $\theta_0 \to \theta_0 + \theta$, so the action is not actually invariant. A very important property of the integral $(e^2/32\pi^2)\int d^4x \mathrm{Tr} F_{\mu\nu}(x)\tilde{F}^{\mu\nu}(x)$ is that, for topological reasons, it is always an integer. If we shift θ_0 by a multiple of 2π, the functional integral is unchanged, $Z' = \exp(i2\pi p)Z = Z$, where p is some integer. We can make such a shift by choosing $\theta = 2\pi p/N_f, p \in \{0, ..., N_f - 1\}$. This reduces the axial symmetry

$$U(1)_A \longrightarrow \mathbf{Z}(N_f). \tag{1.26}$$

However, we also have the chiral symmetry $SU(N_f)_L \otimes SU(N_f)_R$ of N_f massless quark flavors, which is reduced to $SU(N_f)_{L=R}$ by a non-zero expectation value for the quark condensate. As $\mathbf{Z}(N_f) \subset SU(N_f)$, the discrete symmetry which is left over from the broken axial symmetry are already contained in the full or reduced chiral symmetry group. The $U(1)_A$ axial symmetry is completely broken by the anomaly.

SUSY $SU(N)$ Yang-Mills theory is also invariant at the classical level if we make a $U(1)_A$ axial transformation of the gluinos. This symmetry is reduced when we include the quantum anomaly. The coefficient of the Pontryagin density is shifted by $\theta_0 \to \theta_0 + 2N\theta$. The coefficient is shifted by a different amount as the gluinos are in the adjoint, as opposed to fundamental, representation of the gauge group $SU(N)$. If we choose $\theta = n/(2N), n \in \{0, ..., 2N - 1\}$, θ_0 is shifted by a multiple of 2π and the functional integral is invariant. However, such a choice transforms the gluinos non-trivially. This means that the continuous classical axial symmetry is reduced to a discrete chiral symmetry of the full quantum theory,

$$U(1)_A \longrightarrow \mathbf{Z}(2N)_\chi. \tag{1.27}$$

As there is only one flavor of massless gluino, this discrete symmetry is not contained

in any larger chiral symmetry group.

In QCD with N_f massless quarks, the chiral symmetry is reduced when the quark condensate obtains non-perturbatively a non-zero expectation value, which reduces the symmetry $SU(N_f)_L \otimes SU(N_f)_R \rightarrow SU(N_f)_{L=R}$. In SUSY pure gauge theory, the discrete chiral symmetry is reduced when the gluino condensate, $\chi = \langle \Psi^a \Psi_a \rangle$, is non-zero. This breaks the symmetry down to

$$\mathbf{Z}(2N)_\chi \longrightarrow \mathbf{Z}(2)_\chi \tag{1.28}$$

— we can still make the rotation $\Psi'^a = -\Psi^a$ and the gluino condensate is unchanged. This means that a $\mathbf{Z}(N)_\chi$ symmetry is broken by a non-zero value of the gluino condensate. This generates N degenerate bulk phases which are distinguished by their values of χ. Lattice simulations show that discrete chiral symmetry breaking does indeed occur [21].

As well as a discrete $\mathbf{Z}(N)_\chi$ chiral symmetry, SUSY Yang-Mills theory also has the $\mathbf{Z}(N)_c$ center symmetry of non-supersymmetric pure gauge theory. The center symmetry is explicitly broken in QCD by the quarks, which transform under the fundamental representation of the gauge group. However, the gluinos transform under the adjoint representation and do not break the center symmetry. We would like to study the connection between confinement and chiral symmetry breaking in one theory. Non-supersymmetric Yang-Mills theory has an order parameter for a symmetry connected with confinement, but has no chiral symmetry. QCD with massless quarks has chiral symmetry and an associated order parameter, but the symmetry related to confinement is explicitly broken. SUSY Yang-Mills theory has order parameters for both confinement and discrete chiral symmetry. This makes it an interesting theory where we can explore the relationship between these fundamental properties of QCD.

Chapter 2

QCD Strings and SUSY Domain Walls

2.1 Predictions from String Theory

We have already shown that SUSY $SU(N)$ Yang-Mills theory has a discrete $\mathbf{Z}(N)_\chi$ chiral symmetry of axial transformations of the gluinos. This symmetry is broken spontaneously by a non-perturbatively generated expectation value for the gluino condensate χ. Breaking the discrete symmetry produces N distinct degenerate bulk phases, which are distinguished by different complex values of the condensate. These distinct phases are separated by domain walls, very like those produced when the center symmetry of non-supersymmetric Yang-Mills theory is broken.

Using Matrix-theory techniques in String theory, it has been predicted that the domain walls of SUSY Yang-Mills theory interact with the QCD string which carries the color flux [22]. In String theory, the domain wall is a D-brane, which is a surface on which strings can end. By taking a low-energy limit of the String theory, a phenomenon is found for a theory in the universality class of $\mathcal{N} = 1$ SUSY $SU(N)$ Yang-Mills theory. We place a static test quark in a region of confining, chirality broken bulk phase. It emits a QCD string, which can end on a domain wall, even though the domain wall does not contain the fundamental color charge carried by the string. The prediction does not explain where the color flux of the QCD string goes

to or how such a phenomenon is possible.

Although the calculation is done in the context of String Theory, we can describe the formation of confining QCD strings and domain walls using field theory. We use an effective field theory with some essential features, such as global symmetries, of the microscopic supersymmetric theory to explain how this effect might occur. We show that the color flux of the QCD string is actually dissipated in a thin film of deconfined bulk phase at the center of the domain wall. This allows us to make a prediction for the phase structure of SUSY $SU(N)$ Yang-Mills theory. We also examine critical phenomena associated with the domain walls.

We have already discussed field theories at non-zero temperature T, i.e. in Euclidean space-time with a finite extent $\beta = 1/T$ in the periodic time direction. With supersymmetry, physical behavior is unchanged by rotations between bosons and fermions. However, in order to obey the Pauli exclusion principle, fermions must have anti-periodic boundary conditions in the time direction, whereas bosons obey periodic boundary conditions. A finite time extent breaks supersymmetry by distinguishing fermions from bosons. To use supersymmetric properties of the theory, one must work at zero temperature, i.e. infinite time extent. This is where effects such as chiral symmetry breaking can be calculated analytically non-perturbatively. It will turn out that our calculations do not require the supersymmetry to be intact, which allows us to examine the theory at non-zero temperature. Although our methods do not require zero temperature, we will examine this scenario first as there has already been much investigation into the properties of zero temperature domain walls [23]. Afterwards, we examine domain walls at $T \neq 0$, where methods relying on supersymmetry cannot be used. The effective field theory we construct is also simpler at zero than at non-zero temperature.

2.2 Zero temperature domain walls

In SUSY $SU(N)$ Yang-Mills theory at zero temperature, where the supersymmetry has not been broken by temperature, there are N distinct confined bulk phases where

chiral symmetry is broken. These phases are distinguished by their values of the gluino condensate

$$\chi = \langle \Psi^a \Psi_a \rangle \in \mathbb{C}, \quad \chi^{(n)} = \chi_0 \exp(2\pi i n/N), \quad n \in \{1, ..., N\}, \tag{2.1}$$

where χ is a complex composite scalar field. It is argued that, at $T = 0$, there is also a non-Abelian Coulomb phase where chiral symmetry is intact, i.e. $\chi^{(0)} = 0$ [24]. This issue is not yet resolved. In this thesis, we assume that the non-Abelian Coulomb phase does exist. The distinct bulk phases are separated by domain walls, which are topological objects formed by the breaking of a discrete symmetry. Domain walls have a free energy cost proportional to their area, where the constant of proportionality is called the interface tension $\alpha = F/A$. A confined-confined domain wall separating two confined phases with gluino condensates $\chi^{(m)}$ and $\chi^{(n)}$ has an interface tension α_{mn}. It has been shown that the interface tension is constrained by the values of the gluino condensate on either side of the interface [23]

$$\alpha_{mn} \geq \frac{N}{8\pi^2} |\chi^{(m)} - \chi^{(n)}| = \frac{N\chi_0}{8\pi^2} |\exp(2\pi i m/N) - \exp(2\pi i n/N)|. \tag{2.2}$$

If the inequality becomes an equality, then the confined-confined domain wall is a BPS state. This means that the energy of the wall is equal to the central charge of the supersymmetry algebra, which breaks some, but not all of the original supersymmetry. A BPS state is also stable and cannot decay to a lower energy state. There are also confined-Coulomb domain walls, which separate confined and Coulomb bulk phases. These interfaces are BPS states and their interface tension is

$$\alpha_{0n} = \frac{N\chi_0}{8\pi^2}. \tag{2.3}$$

The interface tensions determine the shape of a droplet of Coulomb phase that wets a confined-confined domain wall. As shown in figure 2-1a, such a droplet forms

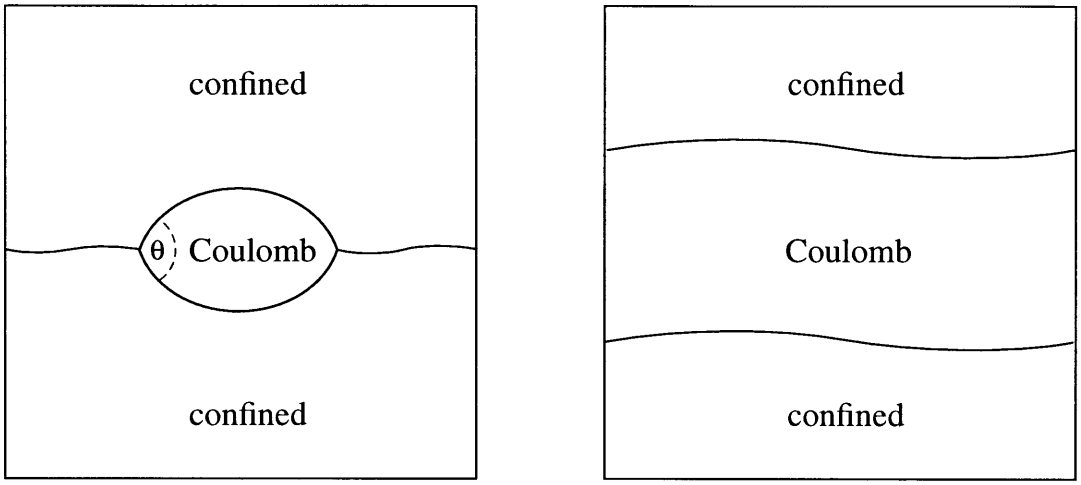

Figure 2-1: *Incomplete versus complete wetting. (a) For $\alpha_{mn} < 2\alpha_{0n}$ one has incomplete wetting with $\theta \neq 0$. Then the Coulomb phase forms a lens shaped droplet at the confined-confined interface. (b) Complete wetting corresponds to $\alpha_{mn} = 2\alpha_{0n}$. Then $\theta = 0$, and the Coulomb phase forms a film that splits the confined-confined domain wall into two confined-Coulomb interfaces.*

a lens with opening angle θ, where

$$\alpha_{mn} = 2\alpha_{0n} \cos\frac{\theta}{2}. \tag{2.4}$$

This equation for θ follows from the forces at the corner of the lens being in equilibrium (forming a stable configuration known as the Neumann triangle in condensed matter literature [25]). In condensed matter physics the inequality

$$\alpha_{mn} \leq 2\alpha_{0n}, \tag{2.5}$$

was derived by Widom and is also known as Antonoff's rule [26]. It follows from thermodynamic stability because a hypothetical confined-confined domain wall with $\alpha_{mn} > 2\alpha_{0n}$ would simply split into two confined-Coulomb interfaces. Combining Antonoff's rule with the BPS inequality, one finds

$$\frac{N\chi_0}{8\pi^2}|\exp(2\pi im/N) - \exp(2\pi in/N)| \leq \alpha_{mn} \leq \frac{N\chi_0}{4\pi^2}. \tag{2.6}$$

Assuming BPS saturation for confined-confined interfaces, the values of the interface tensions from above imply

$$\theta = \pi - \frac{2\pi}{N}(m-n), \text{ for } 1 \leq m-n \leq \frac{N}{2}. \tag{2.7}$$

Then, for odd N, $\theta \neq 0$, such that the Coulomb phase forms droplets at a confined-confined interface. In condensed matter physics this phenomenon is known as incomplete wetting. For even N and for $m-n = N/2$, on the other hand, $\alpha_{mn} = 2\alpha_{0n}$ and $\theta = 0$. In that case, the lens shaped droplet degenerates to an infinite film, as shown in figure 2-1b. When such a film is formed, this is complete wetting.

Wetting phenomena occur frequently in Nature and have been studied in situations such as a liquid-vapor or binary fluid mixture being in contact with a solid wall [13], wetting at grain boundaries [27], in polymer mixtures [28], alloys [29], superconductors [30] and metal vapors [31]. For example, the human eye is completely wet by a film of tears that splits the eye-air solid-gas interface into a pair of solid-liquid and liquid-gas interfaces. Complete wetting may occur when several bulk phases coexist with each other. For condensed matter systems, achieving phase coexistence usually requires fine-tuning of, for example, the temperature, to a first order phase transition. In supersymmetric theories, on the other hand, drastically different phases, like confined and Coulomb, may coexist at zero temperature, since their bulk free energies are identical due to supersymmetry. This implies that complete wetting appears naturally, i.e. without fine-tuning, in supersymmetric theories.

2.3 Critical behavior of complete wetting

Complete wetting is a universal phenomenon of interfaces which occurs at first order phase transitions. Even though such phase transitions have no universal bulk behavior, there are universal properties of the interfaces which are characterized by several critical exponents. For example, the width r of the complete wetting layer separating

the two interfaces diverges as

$$r \propto (T - T_c)^{-\psi}, \tag{2.8}$$

where $T - T_c$ measures the deviation from the point of phase coexistence and ψ is a critical exponent. The value of ψ depends on the range of the interactions between the two interfaces that enclose the complete wetting layer. For condensed matter systems, the interaction energy per unit area is often due to repulsive van der Waals forces and is given by c/r^p. In addition, away from T_c the phase that forms the wetting layer has a slightly larger bulk free energy than the other phases. Close to T_c, the additional bulk free energy per unit area for a wetting layer of width r is given by $\mu(T - T_c)r$. Hence, the total free energy per unit area of the two interface system relative to the free energy of two infinitely separated interfaces at T_c is given by

$$\alpha_{mn}(T) - 2\alpha_{0n}(T_c) = \frac{c}{r^p} + \mu(T - T_c)r. \tag{2.9}$$

Minimizing the free energy with respect to r, one finds the equilibrium width

$$r \propto (T - T_c)^{-1/(p+1)}, \tag{2.10}$$

such that $\psi = 1/(p+1)$. Inserting the equilibrium value of r one finds

$$\alpha_{mn}(T) - 2\alpha_{0n}(T_c) \propto (T - T_c)^{p/(p+1)} \propto (T - T_c)^{1-\psi}. \tag{2.11}$$

Some condensed matter systems with interfaces interact via retarded van der Waals forces with a potential c/r^3, and thus have $\psi = 1/4$ [32]. As we will see, the confined-confined interfaces of SUSY $SU(N)$ pure gauge theory, which are completely wet by the non-Abelian Coulomb phase, have the same critical exponent. This is because, via the massless Coulomb phase, there are long-range interactions between the interfaces.

Complete wetting does not only occur in supersymmetric gauge theories, although only there it occurs naturally without fine-tuning. In fact, Frei and Patkós conjectured that complete wetting occurs in the non-supersymmetric $SU(3)$ pure gauge

theory at the high-temperature deconfinement phase transition [33]. In the deconfined phase the $\mathbf{Z}(3)_c$ center symmetry is spontaneously broken. Hence, there are three distinct high-temperature phases separated by deconfined-deconfined interfaces. When a deconfined-deconfined interface is cooled down to the phase transition, the low-temperature confined phase forms a complete wetting layer. In that case, the interactions between the interfaces are short-ranged, such that

$$\alpha_{mn}(T) - 2\alpha_{0n}(T_c) = a\exp(-br) + \mu(T - T_c)r. \tag{2.12}$$

Minimizing the free energy with respect to r now gives

$$r \propto \ln(T - T_c), \tag{2.13}$$

such that $\psi = 0$. Substituting the value of r, one obtains

$$\alpha_{mn}(T) - 2\alpha_{0n}(T_c) \propto (T - T_c)\ln(T - T_c). \tag{2.14}$$

This is the critical behavior that was observed in ref.[34]. As we will see, the same exponents follow for the high-temperature deconfinement transition in the supersymmetric case. This is because the massive deconfined phase only allows short-range interactions between interfaces.

As argued before, for $\mathcal{N} = 1$ SUSY $SU(3)$ gauge theory (and generally for odd N) complete wetting may occur at zero temperature only if confined-confined domain walls are not BPS saturated. The question as to whether or not these domain walls are BPS states has not yet been answered. At non-zero temperature, we cannot use supersymmetric methods to determine the interface tension. We find that confined-confined interfaces are completely wet by the deconfined phase at high temperature. We will show that complete wetting provides a field theoretic explanation of how a QCD string can end on a domain wall without reference to String Theory.

2.4 Effective theory at zero temperature

2.4.1 Gauge group SU(2)

In SUSY $SU(N)$ gauge theory with even N a confined-confined interface separating phases with gluino condensates $\chi^{(m)}$ and $\chi^{(n)}$ is completely wet by the non-Abelian Coulomb phase if $m - n = N/2$. In this case, Antonoff's rule implies BPS saturation of confined-confined domain walls. The simplest case we can consider is $SU(2)$, where $\chi^{(1)} = -\chi_0$ and $\chi^{(2)} = \chi_0$. The universal aspects of the interface dynamics can be derived from an effective Euclidean action

$$S[\chi] = \int d^4x \, [\frac{1}{2}\partial_\mu\chi\partial_\mu\chi + V(\chi)], \tag{2.15}$$

for the gluino condensate χ. For the effective action to be invariant under the $\mathbf{Z}(2)_\chi$ chiral transformation $\chi \to -\chi$, we require that $V(-\chi) = V(\chi)$. When the two confined phases coexist with the Coulomb phase, $V(\chi)$ has three degenerate minima, two at $\chi = \pm\chi_0$ and one at $\chi = 0$. The confined phase is massive, and thus $V(\chi)$ is quadratic around $\chi = \pm\chi_0$. The Coulomb phase, on the other hand, is massless and $V(\chi)$ turns out to be quartic around $\chi = 0$ [35]. A simple potential with these properties can be written as

$$V(\chi) = \chi^4(a + b\chi^2 + c\chi^4). \tag{2.16}$$

For our purposes it is not essential to use the actual potential of the supersymmetric theory. In fact, the exact effective action for the gluino condensate, which results from integrating out all other fields, is non-local and impossible to compute in practice. We are interested only in the universal complete wetting aspects of the interface dynamics. These are the same for the simple potential from above. The Veneziano-Yankielowicz potential derived from the supersymmetric $SU(N)$ Yang-Mills theory has the form, $V(\chi) = a\chi^4 \ln^2 |\chi/\chi_0|$, and is thus non-analytic for $\chi = 0$ [35]. Indeed, we have verified explicitly that this potential leads to the same critical exponents as the one

from above. It is certainly true that the critical exponents depend on the order of the leading term in the potential (in this case χ^4), but logarithmic corrections and non-analyticities in them do not change this behavior. For $a > 0$ there is a quartic minimum at $\chi = 0$ corresponding to the Coulomb phase. For $0 < a < 9b^2/32c$ and $b < 0$ there are two other minima at

$$\chi_0^2 = \frac{-3b + \sqrt{9b^2 - 32ac}}{8c}, \tag{2.17}$$

corresponding to the two confined phases. Phase coexistence corresponds to $b^2 = 4ac$, because then all three minima are degenerate.

We are interested in the properties of domain walls. We look for solutions of the classical equation of motion representing static planar domain walls, i.e. $\chi(x, y, z, t) = \chi(z)$, where z is the coordinate perpendicular to the wall. The equation of motion then takes the form

$$\frac{d^2\chi}{dz^2} = \frac{dV}{d\chi} = 2\chi^3(2a + 3b\chi^2 + 4c\chi^4). \tag{2.18}$$

To encourage the creation of a domain wall, we choose boundary conditions for χ which force a kink, namely $\chi(\pm\infty) = \pm\chi_0$. If we find such a solution, the interface action per unit area and unit time gives the interface tension α_{mn}.

We solve these classical equations of motion numerically using a computing package called COLSYS [36]. This is a highly efficient method of solving k coupled non-linear ordinary differential equations each of order $m(k)$. It solves the equations iteratively over a finite interval $[-L, L]$ by making a mesh of a finite number of points which are chosen in this interval. COLSYS requires the differential equations, the boundary conditions and the partial derivatives of the kth equation with respect to all derivatives up to order $m(k) - 1$ of all the fields. It also requires an initial guess for the solution of the equations. The points chosen in the interval are not uniformly spaced and, after each iteration, COLSYS chooses a new set of points so that the mesh is most fine in the regions where the solutions are most sensitive. The program iterates until solutions within predetermined tolerances are found and COLSYS re-

turns numerical solutions over the entire interval. This method is extremely quick and far superior to other numerical techniques such as the shooting method.

The critical temperature, where the single Coulomb and the two confined phases coexist, is $T_c = 0$. At T_c, the minima of the effective potential V are degenerate

$$\frac{dV}{d\chi}(\pm\chi_0) = \frac{dV}{d\chi}(0) = 0 \quad \frac{d^2V}{d\chi^2}(\pm\chi_0), \frac{d^2V}{d\chi^2}(0) > 0 \quad V(\pm\chi_0) = V(0). \tag{2.19}$$

This constrains the choice of parameters in the potential to satisfy $b^2 = 4ac$. If we go to a higher temperature $T > T_c$, the two confined phases become degenerate absolute minima and the Coulomb phase becomes a local minimum. This changes one of the constraints to $V(\pm\chi_0) < V(0)$, giving $b^2 > 4ac$. Varying our choice of parameters a, b and c changes how close we are to the critical temperature. Our deviation from criticality is measured by $\Delta = 1 - 4ac/b^2$. Solving the equations of motions at high temperature corresponds to choosing parameters for which the deviation Δ is large, while solutions near criticality correspond to a choice for which Δ is small.

In Figure 2-2, we show a numerical solution of the equation of motion for a domain wall separating the two confined phases with boundary conditions $\chi(\pm\infty) = \pm\chi_0$. Figure 2-2a corresponds to a high temperature where only the confined phase is thermodynamically stable. Then the interface profile interpolates directly between the two confined phases. Figure 2-2b corresponds to an almost zero temperature where the Coulomb phase is metastable. Then the confined-confined domain wall splits into two confined-Coulomb interfaces and the Coulomb phase forms a complete wetting layer between them. Figure 2-3 shows the width r of the complete wetting layer as a function of the deviation Δ from phase coexistence. We determine r numerically as $r = 2z_0$ where the slope of the numerical solution $d\chi/dz$ attains a maximum at $z = z_0$. One finds $r \propto \Delta^{-1/4}$, such that the critical exponent is $\psi = 1/4$. This is the same value that one finds for condensed matter interfaces that interact via long-range retarded van der Waals forces with a potential c/r^3 [32]. We have verified numerically that $\alpha_{mn}(T) - 2\alpha_{0n}(T_c) \propto \Delta^{3/4}$ in agreement with the arguments previously presented. The interface tensions are calculated from the effective action,

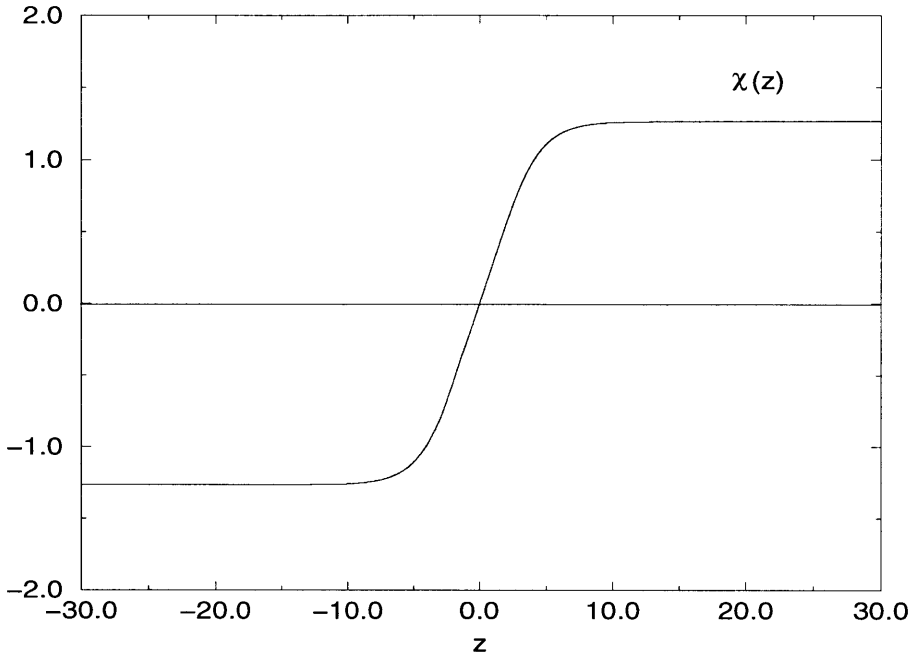

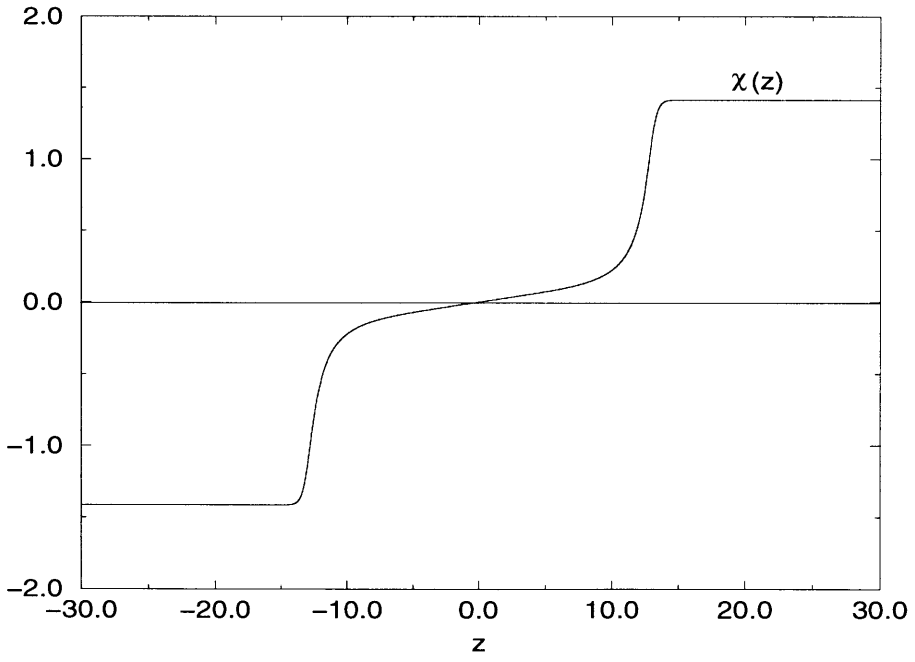

Figure 2-2: *Profile $\chi(z)$ of a confined-confined domain wall for $SU(2)$. (a) At high temperatures the Coulomb phase is unstable, and one goes directly from one confined phase to the other. (b) At almost zero temperature the Coulomb phase is metastable and forms a complete wetting layer that splits the confined-confined domain wall into a pair of confined-Coulomb interfaces.*

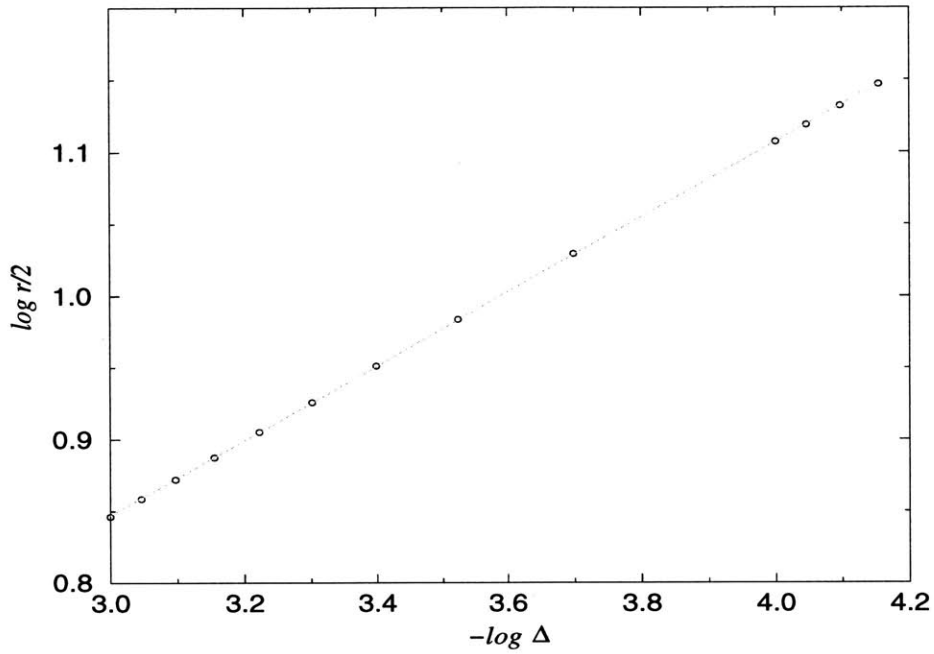

Figure 2-3: *Determination of the critical exponent ψ for $SU(2)$. The straight line in the double-logarithmic plot shows the width of the wetting layer as $r \propto \Delta^{-1/4}$, such that $\psi = 1/4$.*

which we determine numerically. The order parameter at the center of the wetting layer behaves as

$$\frac{d\chi}{dz}(0) \propto \Delta^{1/2}, \tag{2.20}$$

which defines another critical exponent.

The domain walls are classical solutions of the effective action, whose form is governed by symmetry considerations. In statistical mechanical language, this would be a Mean Field theory. We have described the universal behavior of the classical solution near criticality. How is the classical critical behavior affected by quantum fluctuations around the classical solution? It has been shown that, for the interaction of interfaces with long range forces, the upper critical dimension of the theory $d^* < 3$ [32]. At or above this dimension, the Mean Field theory is exact, i.e. the classical solutions contains all the effects of fluctuations. As we are above the critical dimension, we obtain the correct values for the critical exponents. The universal wetting

we observe is unaffected by quantum fluctuations.

We use the simplest effective potential with the required symmetries and whose leading terms around the minima are governed by the phases being massless or massive. The exact effective potential for the gluino condensate at zero temperature has been calculated and the leading term is $a\chi^4 \ln^2 |\chi/\chi_0|$. We stated that, as our effective action has the same symmetries and space-time dimensionality, they occupy the same universality class and have the same critical behavior, which is independent of the details of the potential. This should not be affected by a logarithmic correction to the leading term. To test this universality, we also use an effective potential

$$V(\chi) = a\chi^4 \ln^2 |\chi/\chi_0| + b\chi^6 + c\chi^8 + d\chi^{10}. \tag{2.21}$$

We choose the parameters a, b, c and d in the potential so that the confined, chirality broken phases $\chi = \pm\chi_0$ are absolute minima and the Coulomb, chirality intact phase $\chi = 0$ is a local minimum. Using COLSYS to solve the equations of motion numerically, we find that the confined-confined domain wall is completely wet by the Coulomb phase at $T = 0$ and that the critical exponents describing this critical behavior are the same as for the simpler potential. This verifies the universality of the phenomenon.

For the particular case of $SU(2)$, we can use another method to determine the width of the wetting layer. The Euclidean effective action has only one real field χ. Domain walls appear as planar solutions of the classical equations of motion, so the fields only depend on one coordinate z. The Euclidean energy is

$$E = \int d^4x [\frac{1}{2}\partial_\mu\chi\partial_\mu\chi - V(\chi)], \tag{2.22}$$

which is zero for a solution to the classical Euclidean equations of motion. This means that the integrand is zero, $1/2(d\chi/dz)^2 - V(\chi) = 0$. When we are away from the critical point, the absolute minimum of the effective potential is $V_{min} = V(\pm\chi_0) =$

$V(\chi(z=\pm\infty))$. We integrate this equation to find the complete wetting layer width

$$r = 2z_0, \quad z_0 = \int_0^{z_0} dz = \int_0^{\chi_{max}} \frac{d\chi}{\sqrt{2(V(\chi) - V_{min})}}, \tag{2.23}$$

where χ_{max} is defined by $dV/d\chi(\chi_{max}) = 0$. At this point, V attains a maximum and, as $E = 0$, $d\chi/dz$ is also a maximum, giving us the same definition of r as before. We choose the parameters in the potential V so that the confined phases are absolute minima and the Coulomb phase a local minimum and we perform this integral numerically. The deviation from criticality is determined by our choice of parameters. As we approach the critical point, where the Coulomb phase $\chi = 0$ is degenerate with the confined phase $\chi = \pm\chi_0$, i.e. $V(0) = V_{min}$, the integral diverges. This divergence is simply the width of the wetting layer r becoming infinite. We can use this method to determine r several orders of magnitude closer to T_c, where COLSYS can no longer solve the equations of motion. We find the critical exponent describing the divergence of the wetting layer is $\psi = 1/4$, in exact agreement with the other methods. This inversion to find $z(\chi)$ only works for $SU(2)$ domain walls with one field and one coordinate.

2.4.2 Gauge group SU(3)

Let us now turn to $SU(3)$ SUSY Yang-Mills theory. In that case, complete wetting can occur at zero temperature only if confined-confined domain walls are not BPS saturated. For the following discussion we will assume that they are not. The universal aspects of the interface dynamics are again captured by an effective action

$$S[\chi] = \int d^4x \, [\frac{1}{2}\partial_\mu\chi^*\partial_\mu\chi + V(\chi)], \tag{2.24}$$

but the gluino condensate $\chi = \chi_1 + i\chi_2$ is now a complex field. The effective potential $V(\chi)$ is restricted by $\mathbf{Z}(3)_\chi$ and charge conjugation symmetry. Under chiral transformations $z \in \mathbf{Z}(3)_\chi$, the gluino condensate transforms into $\chi' = \chi z$ and under

charge conjugation it gets replaced by its complex conjugate. This implies

$$V(\chi z) = V(\chi),\ V(\chi^*) = V(\chi). \tag{2.25}$$

Again, one needs the potential to be quadratic around the confined phase minima and quartic around the Coulomb phase minimum. A simple potential with these properties is

$$V(\chi) = |\chi|^2(a|\chi|^2 + b\chi_1(\chi_1^2 - 3\chi_2^2) + c|\chi|^4). \tag{2.26}$$

Note that the term $\chi_1(\chi_1^2 - 3\chi_2^2) = \text{Re}\ \chi^3$, which is clearly $\mathbf{Z}(3)$ invariant. Another $\mathbf{Z}(3)$ invariant term is Im χ^3, i.e. the imaginary part of χ^3, but we do not include this as it is not invariant under complex conjugation. At zero temperature (corresponding to $b^2 = 4ac$), the above potential has four degenerate minima at $\chi = \chi^{(n)} = \chi_0 \exp(2\pi i n/3)$, $n \in \{1, 2, 3\}$, representing the three confined phases and at $\chi = \chi^{(0)} = 0$ representing the Coulomb phase. The Euclidean equations of motion for the real and imaginary parts of the gluino condensate are

$$\frac{d^2\chi_i}{dz^2} = \frac{\partial V}{\partial \chi_i}, i = 1, 2. \tag{2.27}$$

Again, we look for solutions of the classical equations of motion representing planar domain walls, which we solve using COLSYS. Figure 2-4 shows a numerical solution of these equations for a domain wall separating two confined phases with boundary conditions $\chi(\infty) = \chi^{(1)} = (\chi_0/2)(-1 + i\sqrt{3})$, $\chi(-\infty) = \chi^{(2)} = (\chi_0/2)(-1 - i\sqrt{3})$. Figure 2-4a corresponds to a temperature deep in the confined phase. In this case, the Coulomb phase is unstable and the domain wall interpolates directly from one confined phase to the other. Figure 2-4b shows the situation at almost zero temperature. Then the confined-confined domain wall splits into two confined-Coulomb interfaces and the Coulomb phase forms a complete wetting layer between them.

As in the $SU(2)$ case, we have determined the width of the complete wetting layer numerically. Again, one finds $r \propto \Delta^{-1/4}$, such that $\psi = 1/4$. Here, r is defined

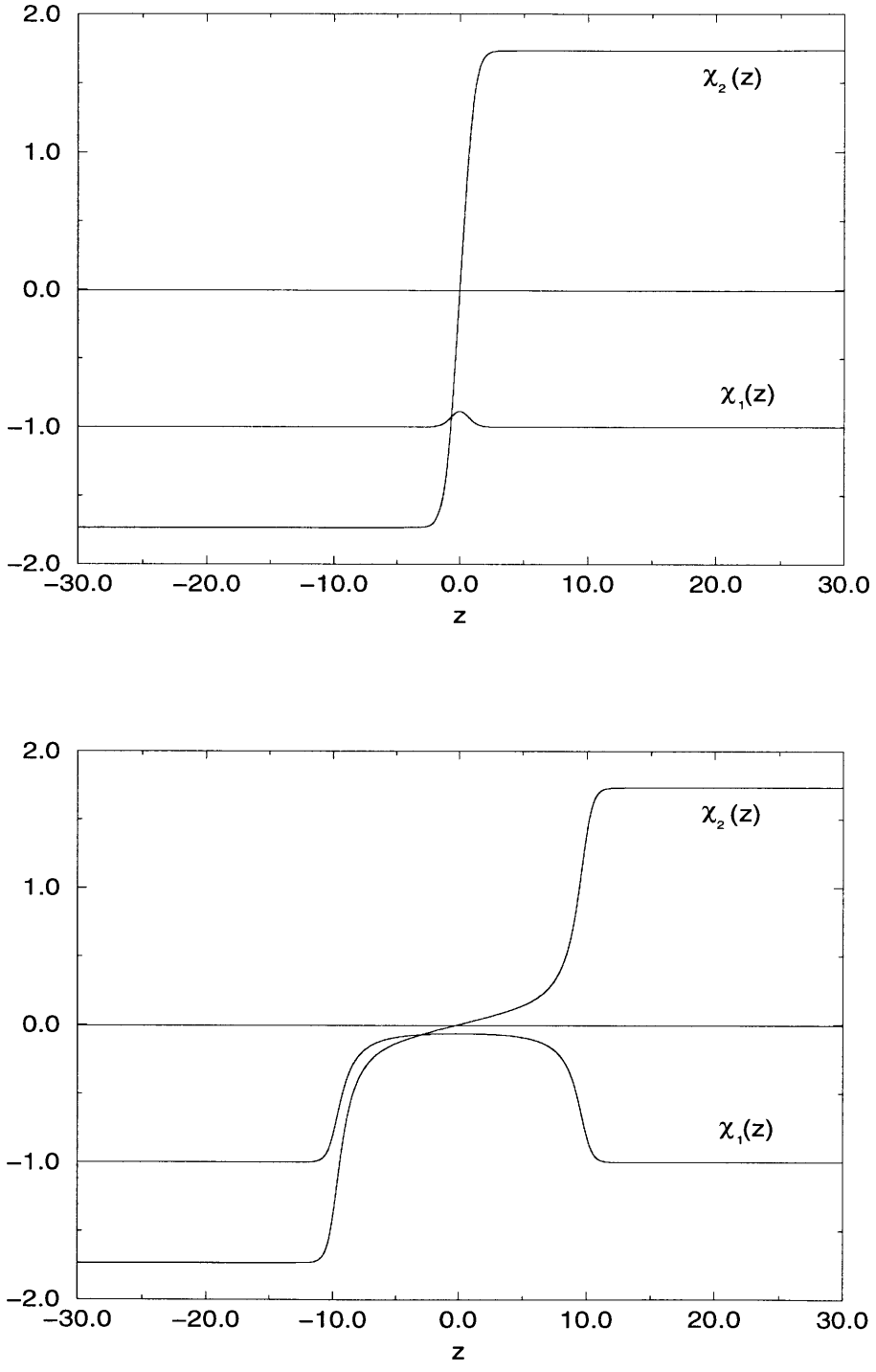

Figure 2-4: *Shape of a confined-confined domain wall for $SU(3)$. (a) Deep in the confined phase the domain wall profile interpolates directly from one confined phase to the other. (b) At almost zero temperature the wall splits into two confined-Coulomb interfaces with a complete wetting layer of Coulomb phase between them.*

as $r = 2z_0$, where $d\chi_2/dz$ attains a maximum at $z = z_0$. In addition, we calculate numerically the action per unit area per unit time and find that the interface tensions behave as $\alpha_{mn}(T) - 2\alpha_{0n}(T_c) \propto \Delta^{3/4}$, as before. The order parameter at the center of the wetting layer now behaves as

$$\chi_1(0) \propto \Delta^{1/4}, \ \frac{d\chi_2}{dz}(0) \propto \Delta^{1/2}, \tag{2.28}$$

again in agreement with the $SU(2)$ critical exponent.

We conclude that the critical exponents are independent of N and depend only on the range of the interface interactions. To summarize, at zero temperature complete wetting occurs for even N and $m - n = N/2$. For odd N or $m - n \neq N/2$ complete wetting can occur only if confined-confined domain walls are not BPS saturated. When a confined-confined domain wall is completely wet by the Coulomb phase, the complete wetting layer grows with the fourth root of the deviation from the critical temperature. This is due to long-range interactions in the Coulomb phase mediated by massless gluons and gluinos (rather than massive glueballs), which lead to $\psi = 1/4$. Of course, it should be noticed that our results are not derived directly from the supersymmetric Yang-Mills theory. Our effective theory does not require supersymmetry to be intact and so we can work at non-zero temperature. An important input from the supersymmetric microscopic theory, which leads to $\psi = 1/4$, is the Veneziano-Yankielowicz potential, whose leading term is quartic. Besides that, our effective theories have the same symmetries as the full theory and should hence be in the same complete wetting universality class. We have varied the form of the potential to check that this assumption of universality holds.

2.5 Effective theory at high temperature

We now discuss the behavior of the domain walls at high temperatures where a phase transition separates the confined phase from a high-temperature deconfined phase. Before we examine the universal properties of domain walls in supersymmetric

theories, we summarize the behavior of interfaces in non-supersymmetric theories.

In the case of non-supersymmetric $SU(3)$ Yang-Mills theory at high temperatures the universal aspects of the interface dynamics are captured by a 3-d effective action [34],

$$S[\Phi] = \int d^3x \, [\frac{1}{2}\partial_i \Phi^* \partial_i \Phi + V(\Phi)], \tag{2.29}$$

for the Polyakov loop Φ, the real part of whose expectation value $\Re\langle\Phi\rangle = \exp(-F/T)$, measures the free energy F of a static quark at temperature T. The Polyakov loop is obtained from integrating over the finite Euclidean time extent $\beta = 1/T$ and so the effective theory is 3-dimensional. In the confined phase, F diverges and $\langle\Phi\rangle$ vanishes, while in the deconfined phase, F is finite and $\langle\Phi\rangle$ is non-zero. Under topologically non-trivial gauge transformations, which are periodic in Euclidean time up to a center element $z \in \mathbf{Z}(3)_c$, the Polyakov loop changes into $\Phi' = \Phi z$. Hence, the $\mathbf{Z}(3)_c$ center symmetry is spontaneously broken in the deconfined phase. Under charge conjugation, the Polyakov loop is replaced by its complex conjugate. The effective potential $V(\Phi)$ is restricted by $\mathbf{Z}(3)_c$ and charge conjugation symmetry, i.e.

$$V(\Phi z) = V(\Phi), \; V(\Phi^*) = V(\Phi), \tag{2.30}$$

as these are symmetries of the microscopic theory. All the phases are massive (note that the deconfined phase has a finite screening length), such that the potential is quadratic around all minima. A simple potential with these properties takes the form

$$V(\Phi) = a|\Phi|^2 + b\Phi_1(\Phi_1^2 - 3\Phi_2^2) + c|\Phi|^4, \tag{2.31}$$

where $\Phi = \Phi_1 + i\Phi_2$. One can restrict oneself to quartic potentials because they are sufficient to explore the universal features of the interface dynamics. At the deconfinement phase transition temperature (corresponding to $b^2 = 4ac$), the above potential has four degenerate minima at $\Phi = \Phi^{(n)} = \Phi_0 \exp(2\pi i n/3)$, $n \in \{1, 2, 3\}$ representing the three deconfined phases and at $\Phi^{(0)} = 0$ representing the confined phase. In ref.[34] it was shown that a deconfined-deconfined domain wall is completely wet by

the confined phase and the corresponding critical exponents have been determined analytically. As expected for short-range forces, one finds $\psi = 0$, i.e. the width of the complete wetting layer diverges logarithmically $r \propto \ln \Delta$, where Δ is the deviation from the critical temperature. In addition, for the order parameter at the center of the wetting layer one obtains $\Phi_1(0) \propto \Delta^{1/2}$ and $d\Phi_2/dz(0) \propto \Delta^{1/2}$.

In SUSY $SU(3)$ Yang-Mills theory, we have at the level of the action, $\mathbf{Z}(3)_\chi$ chiral symmetry, $\mathbf{Z}(3)_c$ center symmetry and charge conjugation symmetry. At low temperatures, the $\mathbf{Z}(3)_\chi$ chiral symmetry is spontaneously broken in the confined phase, where the $\mathbf{Z}(3)_c$ center symmetry is intact. The corresponding order parameter is the complex valued gluino condensate $\chi = \chi_1 + i\chi_2$. Under chiral transformations $z \in \mathbf{Z}(3)_\chi$, the gluino condensate transforms into $\chi' = \chi z$ and under charge conjugation it also gets replaced by its complex conjugate. At high temperatures, one expects chiral symmetry to be restored and — as in the non-supersymmetric theory — the $\mathbf{Z}(3)_c$ center symmetry to be spontaneously broken due to deconfinement. Consequently, the effective action describing the interface dynamics now depends on both order parameters Φ and χ, such that

$$S[\Phi, \chi] = \int d^3x \, [\frac{1}{2}\partial_i \Phi^* \partial_i \Phi + \frac{1}{2}\partial_i \chi^* \partial_i \chi + V(\Phi, \chi)]. \tag{2.32}$$

The most general quartic potential consistent with $\mathbf{Z}(3)_c$, $\mathbf{Z}(3)_\chi$ and charge conjugation now takes the form

$$V(\Phi, \chi) = a|\Phi|^2 + b\Phi_1(\Phi_1^2 - 3\Phi_2^2) + c|\Phi|^4 + d|\chi|^2 + e\chi_1(\chi_1^2 - 3\chi_2^2) + f|\chi|^4 + g|\Phi|^2|\chi|^2. \tag{2.33}$$

We first assume that deconfinement and chiral symmetry restoration occur at the same temperature and that the phase transition is first order. We will explore later the alternative scenarios. Then at criticality, three chirally broken confined phases coexist with three distinct chirally symmetric deconfined phases. The three deconfined phases have $\Phi^{(1)} = \Phi_0 \in \mathbf{R}$, $\Phi^{(2)} = (-1 + i\sqrt{3})\Phi_0/2$ and $\Phi^{(3)} = (-1 - i\sqrt{3})\Phi_0/2$ and $\chi^{(1)} = \chi^{(2)} = \chi^{(3)} = 0$, while the three confined phases are characterized by $\Phi^{(4)} =$

$\Phi^{(5)} = \Phi^{(6)} = 0$ and $\chi^{(4)} = \chi_0 \in \mathbf{R}$, $\chi^{(5)} = (-1+i\sqrt{3})\chi_0/2$ and $\chi^{(6)} = (-1-i\sqrt{3})\chi_0/2$. The phase transition temperature corresponds to a choice of parameters $a, b, ..., g$ such that all six phases $\Phi^{(n)}$, $\chi^{(n)}$ represent degenerate absolute minima of $V(\Phi, \chi)$.

We again look for solutions of the classical equations of motion, representing planar domain walls, i.e. $\Phi(\vec{x}) = \Phi(z)$, $\chi(\vec{x}) = \chi(z)$, where z is the coordinate perpendicular to the wall. The equations of motion then take the form

$$\frac{d^2\Phi_i}{dz^2} = \frac{\partial V}{\partial \Phi_i}, \quad \frac{d^2\chi_i}{dz^2} = \frac{\partial V}{\partial \chi_i}, \quad i = 1, 2. \tag{2.34}$$

As before, we solve these coupled non-linear ordinary differential equations numerically using COLSYS. Figure 2-5 shows a numerical solution of these equations for a domain wall separating two confined phases of type (5) and (6), i.e. with boundary conditions $\Phi(\infty) = \Phi^{(5)}$, $\chi(\infty) = \chi^{(5)}$ and $\Phi(-\infty) = \Phi^{(6)}$, $\chi(-\infty) = \chi^{(6)}$. Figure 2-5a corresponds to a temperature deep in the confined phase. Still, at the domain wall the Polyakov loop is non-zero, i.e. the center of the domain wall shows characteristic features of the deconfined phase. Figure 2-5b corresponds to a temperature very close to the phase transition. Then the confined-confined domain wall splits into two confined-deconfined interfaces and the deconfined phase forms a complete wetting layer between them. The solutions of figure 2-5 have deconfined phase of type (1) at their centers. Due to the $\mathbf{Z}(3)_c$ symmetry, there are related solutions with deconfined phase of types (2) and (3).

For the special values $d = a = 0$, $e = b$, $f = c$, $g = 2c$ we can also find an analytic solution for a confined-deconfined interface. Combining two of these solutions to a confined-confined interface, one obtains

$$\begin{aligned}
\Phi_1(z) &= -\frac{1}{2}\Phi_0[\tanh\alpha(z - z_0) - \tanh\alpha(z + z_0)], \ \Phi_2(z) = 0, \\
\chi_1(z) &= -\frac{1}{4}\chi_0[2 + \tanh\alpha(z - z_0) - \tanh\alpha(z + z_0)], \\
\chi_2(z) &= \frac{\sqrt{3}}{4}\chi_0[\tanh\alpha(z - z_0) + \tanh\alpha(z + z_0)],
\end{aligned} \tag{2.35}$$

where $\Phi_0 = \chi_0 = -3b/4c$ and $\alpha = -3b/4\sqrt{c}$ (with $b < 0$). When $d = a = 0$,

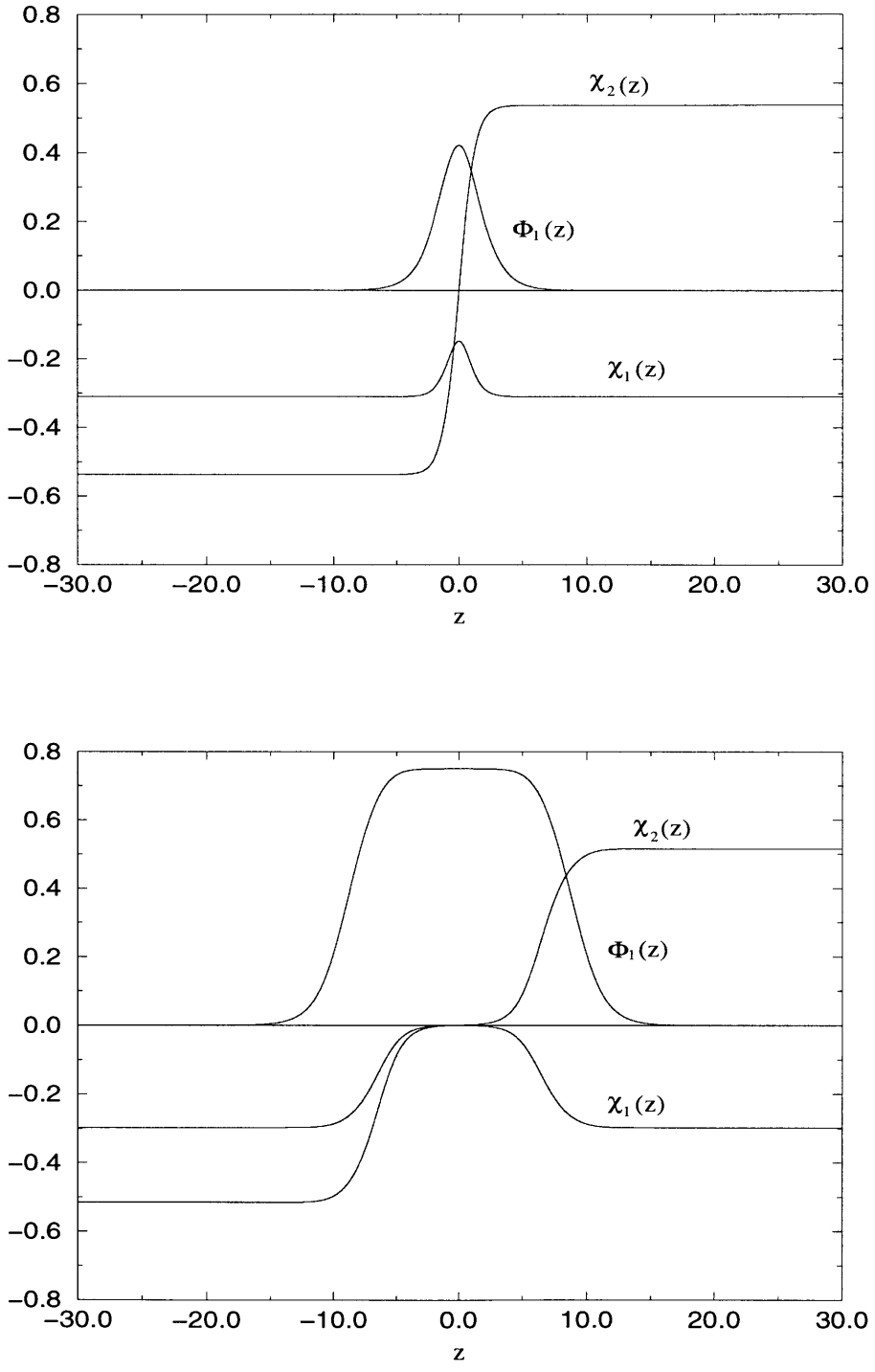

Figure 2-5: *Shape of a confined-confined domain wall for $SU(3)$. (a) Deep in the confined phase $\Phi_1(0) \neq 0$, i.e. the center of the wall has properties of the deconfined phase. (b) Close to the phase transition the wall splits into two confined-deconfined interfaces with a complete wetting layer of deconfined phase between them.*

the critical temperature corresponds to $e^4/f^3 = b^4/c^3$. Near criticality, where $\Delta = e^4/f^3 - b^4/c^3$ is small, the above solution is valid up to order $\Delta^{1/2}$, while now $e = b$ and $f = c$ are satisfied to order Δ. The width of the deconfined complete wetting layer,

$$r = 2z_0 = -\frac{1}{2\alpha} \ln \Delta + C, \tag{2.36}$$

where C is a constant, grows logarithmically as we approach the phase transition temperature. Here, z_0 is determined as the value of z for which $d\chi_2/dz$ attains a maximum. This is the expected critical behavior for interfaces with short-range interactions [34]. We have also checked that $\alpha_{mn}(T) - 2\alpha_{0n}(T_c) \propto \Delta \ln \Delta$, as expected. Again, the order parameter at the center of the wetting layer behaves as

$$\chi_1(0) \propto \Delta^{1/2}, \ \frac{d\chi_2}{dz}(0) \propto \Delta^{1/2}. \tag{2.37}$$

The domain walls at zero temperature interact via long-ranged forces and the upper critical dimension of the Mean Field theory $d^* < 3$. At high temperature, where the domain walls interact via short-ranged forces, it has been shown that the upper critical dimension is $d^* = 3$ [32]. It has also been shown that the universal behavior of complete wetting is correctly described at the critical dimension by the Mean Field theory. This tells us that our classical solutions contain all the effects of quantum fluctuations.

Complete wetting also occurs on the other side of the phase transition. At very high temperatures, we have deconfined-deconfined interfaces separating distinct deconfined phases. As we approach the critical temperature from above, the confined phase completely wets the deconfined-deconfined interfaces. The treatment of this case is completely analogous, and the resulting critical exponents are again those for interfaces with short-range interactions. At zero temperature, we found the same critical behavior of the interfaces for different gauge groups $SU(N)$. We expect the high-temperature interface critical behavior is also independent of N. It would be interesting if complete wetting could be studied in the framework of M-theory. If so, it should correspond to the unbinding of a pair of D-branes, which are tightly bound

in the low-temperature phase.

2.6 Explanation of string ending on wall

Now we wish to explain why the appearance of the deconfined phase at the center of the domain wall allows a QCD string to end there. We recall that an expectation value $\langle\Phi\rangle \neq 0$ implies that the free energy of a static quark is finite. Indeed, the solution of figure 2-5 containing deconfined phase of type (1) has $\Phi_1(0) \neq 0$, such that a static quark located at the center of the wall has finite free energy. Away from the wall centered at $z = 0$, Φ becomes small and the equation of motion for Φ_1 is

$$\frac{d^2\Phi_1}{dz^2} = (2a + 2g|\chi|^2)\Phi_1 + O(|\Phi|^2). \tag{2.38}$$

Solving this, we find that as one moves away from the wall, the Polyakov loop decreases as

$$\Phi_1(z) \propto \exp(-F(z)/T) \propto \exp(-\sqrt{2a + 2g\chi_0^2}\, z). \tag{2.39}$$

Consequently, as the static quark is displaced from the wall, its free energy $F(z)$ increases linearly with the distance z from the center, i.e. the quark is confined to the wall. The string emanating from the static quark ends on the wall and has a tension

$$\sigma = \lim_{z\to\infty} \frac{F(z)}{z} = \sqrt{2a + 2g\chi_0^2}\, T. \tag{2.40}$$

We have solved the classical equations of motion to find the domain wall profile. Still, there are the other domain wall solutions (related to the one from above by $\mathbf{Z}(3)_c$ transformations), which contain deconfined phase of types (2) and (3). One could argue that, after path integration over all domain wall configurations, the quantum domain wall solution has $\langle\Phi\rangle = 0$ at its center. However, this is not true. In fact, the wetting layer at the center of a confined-confined domain wall is described by a two-dimensional field theory with a spontaneously broken $\mathbf{Z}(3)_c$ symmetry. Consequently, deconfined phase of one definite type spontaneously appears at the domain wall. This

argument does not apply to an interface of finite area, e.g. to a bubble wall enclosing a finite volume of confined phase of type (5) in a Universe filled with confined phase of type (4). Indeed, due to quantum tunneling the deconfined wetting layer at the surface of such a bubble would change from type (1) to types (2) and (3). As a consequence, $\langle \Phi \rangle = 0$, such that a QCD string cannot end at the bubble wall. This observation is consistent with the $\mathbf{Z}(3)_c$ Gauss law applied to the compact surface of the bubble. Color flux entering the bubble through a string must exit it somewhere else and then go to infinity. Therefore, the static quark at the origin of the string has infinite free energy and is confined in the usual sense. The deconfined wetting layer of an infinite domain wall, on the other hand, can transport flux to infinity at a finite free energy cost. Thus, a static quark at a finite distance from the wall has a finite free energy and the string emanating from it can end on the wall. The above arguments imply that a QCD string can also end at a confined-deconfined interface at the high-temperature phase transition. This is possible even in non-supersymmetric Yang-Mills theory.

We now understand that QCD strings can end on a confined-confined domain wall provided it is completely wet by deconfined phase. So far we have assumed that, above the phase transition, confinement is lost and simultaneously chiral symmetry is restored, i.e. $T_c = T_\chi$. In that case, indeed there is complete wetting. Now let us consider the two alternative scenarios for the phase transition. First, we assume that chiral symmetry is still restored at temperatures above the phase transition, but that the theory remains confining, i.e. $T_\chi < T_c$. In that case, complete wetting still occurs as we approach T_χ, but now the wetting layer consists of chirally symmetric confined phase, which has $\Phi = 0$. We show this scenario in Figure 2-6 (a). Under these conditions, a QCD string could not end on the wall.

Alternatively, we assume that, above the phase transition, the theory is deconfined, but that chiral symmetry remains broken. In this deconfined, chirality broken phase, both Φ and χ are non-zero, so there are in total nine high-temperature phases. Assuming that the gluino condensate does not vary drastically across the transition, one can show that complete wetting does not occur as we approach T_c. Hence, again

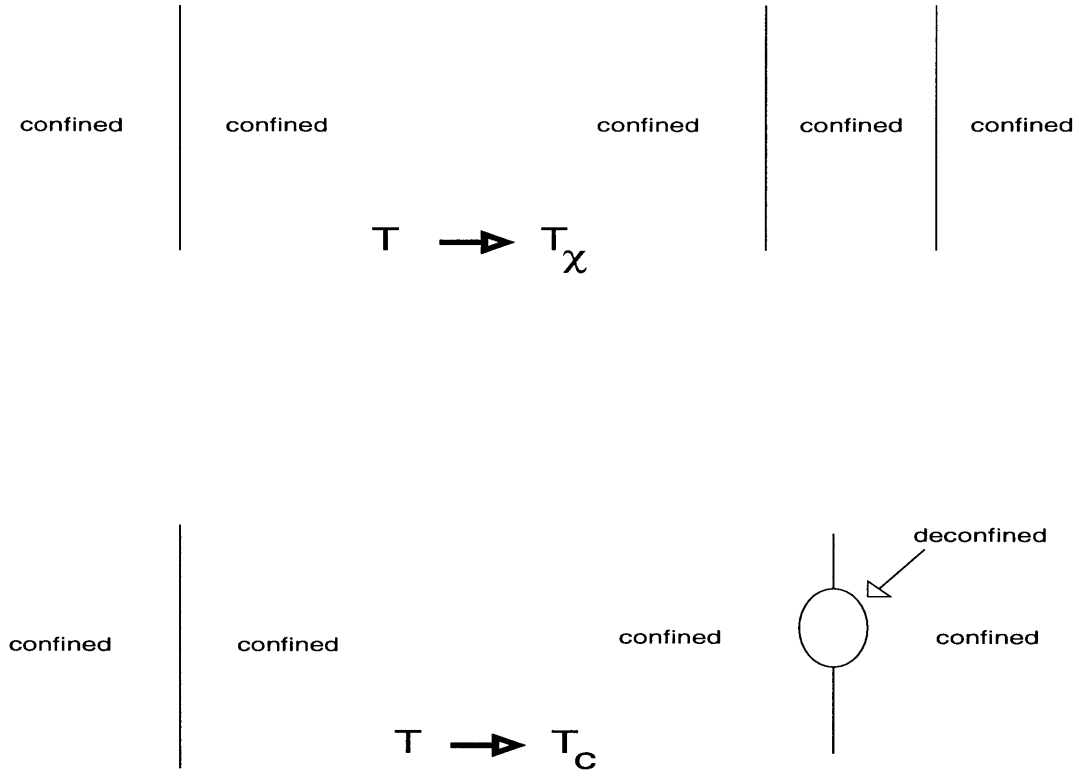

Figure 2-6: *Possible alternatives for the phase transitions: (a) $T_\chi < T_c$ — a domain wall between confined, chirality broken phases is completely wet by a film of confined, chirality restored phase (b) $T_c < T_\chi$ — the domain wall is incompletely wet by bubbles of deconfined, chirality broken phase.*

$\Phi = 0$ at the center of the domain wall and a QCD string could not end there. It should be noted that a confined-confined domain wall could still be incompletely wet, i.e. droplets of deconfined phase could appear at the wall. We show this scenario in Figure 2-6 (b). Even in that case, a QCD string cannot end at a droplet. In contrast to a complete wetting layer, a droplet has a finite volume. Hence, due to quantum tunneling a deconfined droplet of type (1) will turn into one of types (2) and (3). As a result, the average Polyakov loop vanishes for these configurations, and a static quark has infinite free energy even close to the wall. Given that QCD strings can end on the walls, as explained by Witten, we conclude that the two alternative scenarios for the phase transition can be ruled out. Interestingly, Witten's M-theory arguments in combination with our results for complete wetting suggest that SUSY $SU(N)$ Yang-Mills theory has a high-temperature phase transition in which simultaneously

confinement is lost and chiral symmetry is restored.

The width of the complete wetting layer r diverges logarithmically as we approach the critical temperature T_c. If we reduce the temperature, the wetting layer shrinks. We assume that the width does not vanish at some temperature above zero. Then the layer, although microscopic, still exists at zero temperature. Then we can connect our high temperature explanation of how a QCD string ends on a domain wall with the calculation in the supersymmetric gauge theory at zero temperature. It is quite natural for this to occur, but we cannot rule out the possibility that the layer disappears at some other non-zero critical temperature.

There has been much work on the phase structure of theories similar to these. Numerical studies for SUSY $SU(2)$ Yang-Mills theory show that the discrete chiral symmetry is broken non-perturbatively [21]. There has also been study into $SU(3)$ QCD with 2 flavors of massless Dirac fermions which are in the adjoint representation of the gauge group [37]. This quantum theory has $\mathbf{Z}(3)_c$ center symmetry and $SU(2)_L \otimes SU(2)_R$ chiral symmetry. This work has shown that deconfinement and the breaking of continuous chiral symmetry occur at different temperatures. SUSY $SU(3)$ Yang-Mills theory can also be described as QCD with $1/2$ of a flavor of massless adjoint Dirac fermions, which has not yet been fully investigated numerically.

2.7 Summary

We have investigated universality classes for complete wetting in SUSY $SU(N)$ Yang-Mills theory. At zero temperature, the Coulomb phase may completely wet a confined-confined interface. In that case the interfaces interact via long-range forces. The corresponding critical exponents are the same as those for condensed matter systems with retarded van der Waals forces with a c/r^3 potential. One should keep in mind that we have assumed that the Coulomb phase indeed exists in supersymmetric Yang-Mills theory and that its basic characteristics are correctly described by the Veneziano-Yankielowicz potential. Should this not to be the case, our calculation, of course, does not apply to this theory. Even then, it still correctly describes the effective theories

discussed here.

We have also investigated $\mathbf{Z}(3)_c \otimes \mathbf{Z}(3)_\chi$ symmetric effective theories for the Polyakov loop and the gluino condensate at high temperatures. As we approach the critical temperature from below, the massive deconfined phase completely wets a confined-confined interface, and the interactions between interfaces are short-ranged. Then the width of the complete wetting layer grows logarithmically as one approaches T_c. Above T_c, the confined phase can wet a deconfined-deconfined domain wall, with the same critical exponents as before. In general, at zero and high temperatures, the critical exponents are independent of N and depend only on the range of the interface interactions.

Due to complete wetting, deconfined phase appears at a confined-confined domain wall at high temperature. Thus, close to the wall a static quark has a finite free energy and its string can end there. This is possible only when the wall is infinitely extended, because only then it can transport the quark's color flux to infinity at a finite energy cost. Hence, without reference to M-theory, we can understand why a QCD string can end on the wall. Assuming that the phenomenon of the QCD string ending on the interface can occur, we predict the phase structure of SUSY $SU(N)$ Yang-Mills theory. We predict that deconfinement and chiral symmetry restoration happen at the same temperature. This claim remains to be investigated by numerical studies of the supersymmetric theory.

Chapter 3

Confinement in the Deconfined Phase

3.1 Physicality of interfaces

We have already mentioned that when the Early Universe was very hot and dense, the quarks and gluons lived in a plasma of deconfined phase. As the Universe expanded and cooled, there was a phase transition to hadronic matter in a confined phase. In a hypothetical Universe containing only gluons and no quarks, the global $\mathbf{Z}(3)_c$ center symmetry of $SU(3)$ pure gauge theory is spontaneously broken in the deconfined phase and intact in the confined phase. In the very early stages of such a Universe, there would have been three distinct deconfined bulk phases. This Universe would have consisted of many domains of different deconfined phases, the size of each domain being determined via the Kibble mechanism [38]. The domains would have been separated by domain walls. As hadronic matter would have been formed during the Yang-Mills phase transition, the domain wall network might leave some large-scale structure behind. In the real Universe with full QCD, the center symmetry is explicitly broken by the quarks. This singles out one of the deconfined phases as being most energetically favorable and the domain walls become unstable. The interfaces would decay long before the QCD phase transition would occur.

Lattice simulations of pure gauge theory are frequently performed and it is of

much interest to understand the behavior of the domain walls in this context. Also, the interface tension of confined-deconfined domain walls formed at criticality in the pure gauge theory gives as estimate of the magnitude of energy required to form a quark-gluon plasma, which is currently a very active area of experimental research.

The deconfined domain walls are physical objects which exist in Minkowski space-time. In lattice simulations of Yang-Mills theories, interfaces between distinct bulk phases are observed. However, these studies investigate the gauge theory in Euclidean space-time, so that the weight of each possible field configuration in the partition function can be interpreted as a positive Boltzmann probability. It has been debated whether or not the interfaces observed in the numerical studies correspond to the physical domain walls [39]. For example, instantons which exist as local minima of the Euclidean action have no Minkowski space-time counterpart.

To examine the deconfinement phase transition, we look at the behavior of the theory in finite volumes with chosen boundary conditions. We show what effect this has on the phase transition. We calculate the finite volume free energy of a single static quark in particular volumes. We find that even in the high temperature deconfined bulk phase, a static test quark can still be confined, provided the Universe is cylindrical with particular boundary conditions. This relates the free energy of the quark to the interfaces of the Euclidean theory. We argue that this is evidence that these interfaces are physical objects. From the finite volume formulae, we develop a new technique which allows us to extract information about the energy cost of these interfaces.

3.2 Phase transitions in finite volumes

We consider $SU(3)$ pure gauge theory in 4-dimensional Euclidean space-time at non-zero temperature T, i.e. with finite extent $\beta = 1/T$ is the periodic time direction. We are only interested in the confining/deconfining behavior of this theory. We extract this from the Polyakov loop $\Phi(\vec{x})$, which is related to the free energy of a single static test quark by $\mathrm{Re}\langle\Phi\rangle = \exp(-\beta F)$. In the confined phase, F diverges, $\langle\Phi\rangle = 0$

and the $\mathbf{Z}(3)_c$ center symmetry is intact. In the deconfined phase, F remains finite, $\langle\Phi\rangle \neq 0$ and the center symmetry is broken. The spontaneous breaking of the center symmetry is the deconfinement phase transition and is of first order, as would be expected from the breaking of a $\mathbf{Z}(3)$ symmetry.

In lattice simulations of a theory, continuous space-time is discretized into a lattice of a finite number of space-time points. In this lattice, all observables will be analytic functions of the finite number of degrees of freedom. A phase transition is signalled by non-analytic behavior in some observable, which requires the number of degrees of freedom to become infinite. In lattice simulations, we can only observe a true phase transition in the infinite volume limit. At finite volumes, the spontaneous symmetry breaking is sensitive to the spatial boundary conditions — the time direction at non-zero temperature is always periodic — and to the way in which the infinite volume limit is approached. Here, we consider spatial volumes of size $L_x \times L_y \times L_z$. If we choose all spatial directions to be periodic, we find that the expectation value of the Polyakov loop vanishes even in the deconfined phase. This is a consequence of the Gauss law in a periodic volume [40]. A torus has no boundary, so the integral of the flux through the boundary must be zero, so the total charge contained in the torus is zero. The Polyakov loop $\Phi(\vec{x})$ represents a single static quark at $\vec{x}$. As the volume is periodic is every direction, the center electric flux of the quark cannot go to infinity. It can only end in an anti-quark such that the total system is $\mathbf{Z}(3)$ neutral. We cannot have a single quark in a periodic box.

We use a different choice of boundary condition known as C-periodic boundary conditions [41]. If a field is C-periodic in say the z-direction with period L_z, when we translate by this amount in this direction, the field is replaced by its charge conjugate. For example, C-periodic gluons satisfy

$$A_\mu(\vec{x} + L_z\vec{e}_z, t) = A_\mu(\vec{x}, t)^*. \tag{3.1}$$

Here $*$ denotes complex conjugation. We are allowed to make this choice of boundary condition because the action is invariant under charge conjugation. This means that

the system is still translationally invariant. The allowed gauge transformations, as well as the Polyakov loop, also satisfy C-periodicity

$$g(\vec{x} + L_z\vec{e}_z, t) = g(\vec{x}, t)^*, \ \Phi(\vec{x} + L_z\vec{e}_z) = \Phi(\vec{x})^*. \tag{3.2}$$

This is a useful boundary condition for the Polyakov loop. A single quark in a volume now has a partner anti-quark on the other side of the C-periodic boundary. The quark's center electric flux can escape the volume and end on its charge conjugate partner on the other side of the boundary. This allows us to have a single quark in a periodic volume.

The $\mathbf{Z}(3)$ center symmetry is explicitly broken if we apply C-periodicity in any spatial direction [42]. Let us choose the z-direction to be C-periodic. If we twist the gauge group elements as they are shifted by one period in the time direction, $g(\vec{x}, t + \beta) = g(\vec{x}, t)z, z \in \mathbf{Z}(3)$, we find

$$g(\vec{x}, t)^* = g(\vec{x}, t + \beta)^* z = g(\vec{x} + L_z\vec{e}_z, t + \beta)z = g(\vec{x} + L_z\vec{e}_z, t)z^2 = g(\vec{x}, t)^* z^2. \tag{3.3}$$

Consistency requires $z^2 = 1$ and, as $z \in \mathbf{Z}(3)$, then $z = 1$. We no longer have the freedom to twist the gauge transformations, the center symmetry is broken. As we take the infinite volume limit, the bulk becomes less and less sensitive to the boundary conditions and we recover the center symmetry. If we apply C-periodicity in any direction, $\langle\Phi\rangle$ is always non-zero in any finite volume, as $\mathbf{Z}(3)_c$ is explicitly broken by the boundary conditions. In the low temperature confined phase, $\langle\Phi\rangle \to 0$ in the infinite volume limit, while in the high-temperature deconfined phase, $\langle\Phi\rangle$ tends to a non-zero value in the same limit. C-periodic boundary conditions are well-suited for studying the free energy of a single quark, while with periodic boundary conditions a single quark cannot even exist.

We calculate the free energy of a single static quark in a cylindrical volume which is periodic in the short transverse spatial directions and C-periodic in the long direction. In this geometry, we extract interesting behavior in both the confined and deconfined phases.

3.3 Quark free energy in confined phase

The gluon system is known to have a first order phase transition [10] at a temperature T_c. First, we consider the system in the confined phase at temperatures $T < T_c$ in a cylindrical volume with cross section $A = L_x L_y$ and length $L_z \gg L_x, L_y$. Diagrammatically, the partition function is

$$Z = \boxed{\qquad c \qquad} = \exp(-\beta f_c A L_z), \tag{3.4}$$

where f_c is the temperature-dependent free energy density in the confined phase. The expectation value of the Polyakov loop (times Z), on the other hand, is given by

$$Z\langle\Phi\rangle = \boxed{\text{——— } c \text{ ———}} = \exp(-\beta f_c A L_z)\Sigma_0 \exp(-\beta\sigma L_z), \tag{3.5}$$

where σ is the string tension, which is again temperature-dependent, σL_z is the free energy cost of the QCD string and Σ_0 is a constant. The static quark carrys color charge and, in confined phase, the color flux in contained in a QCD string. The confining string (denoted by the additional line in the diagram) connects the static quark with its anti-quark partner on the other side of the C-periodic boundary. Hence, the free energy of the quark is given by

$$F = -\frac{1}{\beta}\ln\Sigma_0 + \sigma L_z. \tag{3.6}$$

As $L_z \to \infty$, the quark is pulled infinitely far apart from its partner anti-quark on the other side of the C-periodic boundary. In this limit, the free energy diverges, telling us the quark is confined, as expected.

In lattice simulations in periodic volumes, the string tension σ can be extracted from measurements of the Wilson loop expectation value $\langle W(R,T)\rangle$ for various R and T. At non-zero temperature, the string tension can also be extracted from the Polyakov loop correlator expectation values $\langle\Phi(\vec{x})\Phi(\vec{y})\rangle \approx \exp(-\beta\sigma|\vec{x}-\vec{y}|)$. In a periodic volume of size L, the maximum spatial extent of the Wilson loop or separation

of the Polyakov loops is $L/2$. In a C-periodic volume, we can extract σ by measuring $\langle\Phi\rangle$ in cylinders of various lengths. The Polyakov loop is a single number and much easier to determine numerically than correlators. If the volume is of size L, the separation between quark and anti-quark is also L, so we probe the potential $V(R)$ between the quarks up to larger distances, even though we work in the same sized volume. We have not yet intensively explored this method of measuring σ in lattice simulations of $SU(3)$ pure gauge theory. It remains to be seen if it is an improvement on standard methods.

3.4 Quark free energy in deconfined phase

We now consider the deconfined phase at temperatures $T > T_c$, where three distinct deconfined phases coexist. They are distinguished by different values for the Polyakov loop and are related to each other by $\mathbf{Z}(3)$ transformations. The expectation values of the Polyakov loop in the three phases are

$$\Phi^{(1)} = (\Phi_0, 0),\ \Phi^{(2)} = (-\frac{1}{2}\Phi_0, \frac{\sqrt{3}}{2}\Phi_0),\ \Phi^{(3)} = (-\frac{1}{2}\Phi_0, -\frac{\sqrt{3}}{2}\Phi_0). \tag{3.7}$$

In a cylindrical volume, a typical configuration consists of several bulk phases, aligned along the z-direction, separated by deconfined-deconfined interfaces. The interfaces cost free energy F proportional to their area A, such that their interface tension is given by $\alpha_{dd} = F/A$. The configurations with more interfaces have a higher energy cost and therefore a smaller Boltzmann weight in the partition function, but they also have a greater entropy as there are many positions in which the interfaces can appear. What matters in the following is the cylindrical shape, not the magnitude of the volume. In fact, our cylinders can be of macroscopic size. The expectation value of the Polyakov loop in a cylindrical volume can be calculated from a dilute gas of interfaces [43]. We write down a series of terms, ordered by the number of interfaces they contain. We assume that the interfaces are dilute, i.e. do not interact. The

interface expansion of the partition function can be viewed as

$$Z = \boxed{d_1} + \boxed{d_2}\boxed{d_3} + \boxed{d_3}\boxed{d_2} + \ldots \tag{3.8}$$

Deconfined phase of type d_i has the value $\Phi^{(i)}$ for the Polyakov loop. The first term has no interfaces and thus the whole cylinder is filled with deconfined phase d_1 only. An entire volume filled with either phase d_2 or d_3 would not satisfy the boundary conditions. The second and third terms have one interface separating phases d_2 and d_3. Due to C-periodicity, we cannot have a configuration with one interface which contains phase d_1. We write down all possible configurations of all possible numbers of interfaces, which gives the series

$$\begin{aligned} Z &= \exp(-\beta f_d A L_z) \\ &+ 2\int_0^{L_z} dz\ \exp(-\beta f_d A z)\gamma \exp(-\beta \alpha_{dd} A) \exp(-\beta f_d A(L_z - z)) + \ldots \\ &= \exp(-\beta f_d A L_z)[1 + 2\int_0^{L_z} dz \gamma \exp(-\beta \alpha_{dd} A) + \ldots] \\ &= \exp(-\beta f_d A L_z)[1 + 2\gamma \exp(-\beta \alpha_{dd} A) L_z + \ldots]. \end{aligned} \tag{3.9}$$

The first term is the Boltzmann weight of deconfined phase of volume AL_z with a free energy density f_d. The second term contains two of these bulk Boltzmann factors separated by an interface contribution $\gamma \exp(-\beta \alpha_{dd} A)$, where γ is a factor resulting from capillary wave fluctuations of the interface. Note that in three dimensions, γ is to leading order independent of the area A [44]. In the above expression, we have integrated over all possible locations z of the interface. As we can take out a factor of the bulk free energy density from all terms, it is straightforward to sum the interface expansion to all orders, giving

$$Z = \exp(-\beta f_d A L_z + 2\gamma \exp(-\beta \alpha_{dd} A) L_z). \tag{3.10}$$

To calculate the expectation value of the Polyakov loop, we use the same interface expansion. For each configuration, we sum the values of Φ in each domain in the

cylinder. In a particular configuration of n interfaces, each domain $k = 1, ..., n+1$ of length L_k (where $\sum_k L_k = L_z$) containing phase $\Phi^{(k)}$ makes a contribution $\Phi^{(k)} L_k / L_z$ to this sum. The total is multiplied by the bulk free energy density weight and the weight of having n interfaces and again we integrate over all possible interface positions.

The series we obtain for the Polyakov loop expectation value is

$$\begin{aligned} Z\langle\Phi\rangle &= \exp(-\beta f_d A L_z)\{\Phi^{(1)} + \int_0^{L_z} dz\ \gamma \exp(-\beta\alpha_{dd}A) \\ &\times \frac{1}{L_z}[\Phi^{(2)} z + \Phi^{(3)}(L_z - z) + \Phi^{(3)} z + \Phi^{(2)}(L_z - z)] + ...\} \\ &= \Phi_0 \exp(-\beta f_d A L_z)\{1 - \gamma \exp(-\beta\alpha_{dd}A) L_z + ...\}. \end{aligned} \tag{3.11}$$

Summing the whole series and dividing by Z, one obtains

$$\langle\Phi\rangle = \Phi_0 \exp(-3\gamma \exp(-\beta\alpha_{dd}A) L_z). \tag{3.12}$$

Note that $\langle\Phi\rangle$ is real, as it should be. The free energy of a static quark in a C-periodic cylinder is therefore given by

$$F = -\frac{1}{\beta} \ln \Phi_0 + \frac{3\gamma}{\beta} \exp(-\beta\alpha_{dd}A) L_z. \tag{3.13}$$

This result is counter intuitive. Although we are in the deconfined phase, the quark's free energy diverges in the limit $L_z \to \infty$, as long as the cross section A of the cylinder remains fixed. This is the behavior one typically associates with confinement. In fact,

$$\sigma' = (3\gamma/\beta) \exp(-\beta\alpha_{dd}A) \tag{3.14}$$

plays the role of the "string tension", even though there is no physical string that connects the quark with its anti-quark partner on the other side of the C-periodic boundary. Confinement in C-periodic cylinders arises because disorder due to many differently oriented deconfined phases destroys the correlations of center electric flux between quark and anti-quark.

Of course, this paradoxical confinement mechanism is due to the cylindrical geometry and the specific boundary conditions. Had we chosen C-periodic boundary conditions in all directions, the deconfined phases d_2 and d_3 would be exponentially suppressed, so that the entire volume would be filled with phase d_1 only. In that case, the free energy of a static quark is $F = -(1/\beta) \ln \Phi_0$, which does not diverge in the infinite volume limit, as expected. Had we worked in a cubic volume, a typical configuration would have no interfaces, the whole volume would be filled with deconfined phase d_1 and again the free energy of a static quark would be $F = -(1/\beta) \ln \Phi_0$. Finally, we note that, in a cylindrical volume, even the static Coulomb potential is linearly rising with a "string tension" e^2/A. This trivial form of confinement is simply due the electric field lines being restricted to the volume, giving a uniform electric field and a potential proportional to the cylinder length. Due to Debye screening, the potential in the deconfined phase $V(R) = \exp(-R/R_D)/R$ falls off much faster than the Coulomb potential, so this trivial confinement effect is absent in the gluon plasma.

Our result implies that deconfined-deconfined interfaces are more than just Euclidean field configurations. In fact, they can lead to a divergence of the free energy of a static quark and thus they have physically observable consequences. Of course, the issue is somewhat academic. First of all, the existence of three distinct deconfined phases relies on the $\mathbf{Z}(3)$ symmetry, which only exists in a pure gluon system — not in the real world with light dynamical quarks. Secondly, the effect is due to the cylindrical geometry and our choice of boundary conditions. Even though it is not very realistic, this set-up describes a perfectly well-defined Gedanken-experiment, demonstrating the physical consequences of deconfined-deconfined interfaces.

The effective "string tension" σ' depends exponentially on the interface tension α_{dd} of a deconfined-deconfined domain wall. If we can observe the finite volume dependence of $\langle \Phi \rangle$ in a numerical examination of the pure gauge theory, we could extract the value of the interface tension. In Chapter 4, we do exactly that in an effective theory of $SU(3)$ Yang-Mills theory. This is a new technique to extract interface tensions from numerical lattice simulations.

3.5 Quark free energy near the phase transition

3.5.1 Complete wetting

We now investigate how the paradoxical confinement mechanism turns into the ordinary one as we lower the temperature to $T \approx T_c$. Since the phase transition is of first order, around T_c, the three deconfined phases coexist with the confined phase. Then, there are also confined-deconfined interfaces with an interface tension α_{cd}. As we have previously discussed, we can have either complete or incomplete wetting of the deconfined-deconfined domain walls. If $\alpha_{dd} = 2\alpha_{cd}$ at $T = T_c$, a deconfined-deconfined interface is unstable and splits into a pair of confined-deconfined interfaces. A film of confined phase grows to macroscopic size and completely wets the deconfined-deconfined interface. Note that $\alpha_{dd} > 2\alpha_{cd}$ is not possible in thermal equilibrium. Thus, the condition for complete wetting does not require fine-tuning. Alternatively, if $\alpha_{dd} < 2\alpha_{cd}$, then incomplete wetting occurs. In that case, both confined-deconfined and deconfined-deconfined interfaces are stable. Instead of a complete layer, bubbles of confined phase form on a deconfined-deconfined interface. Numerical simulations indicate that complete wetting is realized in the gluon system [45, 43]. We calculate the quark free energy in both scenarios.

We first assume that complete wetting occurs. The dilute interface expansion for the partition function takes the form

$$Z = \boxed{c} + \boxed{d_1}$$

$$+ \sum_i \{ \boxed{c}\boxed{d_i}\boxed{c} + \boxed{d_i}\boxed{c}\boxed{d_i^*} \} + \ldots \qquad (3.15)$$

The sum over i extends over the three deconfined phases and d_i^* denotes the charge-conjugate of d_i, i.e. $d_1^* = d_1$ and $d_2^* = d_3$. Note that due to complete wetting, one always has an even number of interfaces. The diagrammatic terms from above give

$$Z = \exp(-\beta f_c A L_z) + \exp(-\beta f_d A L_z)$$

$$+ \quad 3\int_0^{L_z} dz_1 \int_{z_1}^{L_z} dz_2 \; \{ \exp(-\beta f_c A z_1)\delta \exp(-\beta\alpha_{cd}A) \exp(-\beta f_d A(z_2 - z_1))$$
$$\times \quad \delta \exp(-\beta\alpha_{cd}A) \exp(-\beta f_c A(L_z - z_2)) \; + \; \exp(-\beta f_d A z_1)\delta \exp(-\beta\alpha_{cd}A)$$
$$\times \quad \exp(-\beta f_c A(z_2 - z_1))\delta \exp(-\beta\alpha_{cd}A) \exp(-\beta f_d A(L_z - z_2))\} + ... \qquad (3.16)$$

Again, there is a factor for every bulk phase and for every interface. The capillary wave fluctuations of a confined-deconfined interface are characterized by the factor δ. Note that now we integrate over the positions z_1 and z_2 of the two interfaces. It is more convenient to extract an overall bulk factor and write the series as

$$Z = \{ \exp(-\beta(f_c + f_d)AL_z/2)\} \; \{ \; \exp(-xL_z) + \exp(xL_z) + \qquad (3.17)$$
$$3\int_0^{L_z} dz_1 \int_{z_1}^{L_z} dz_2 [\exp(-xz_1)\delta' \exp(x(z_2 - z_1))\delta' \exp(-x(L_z - z_2)) +$$
$$\exp(xz_1)\delta' \exp(-x(z_2 - z_1))\delta' \exp(x(L_z - z_2))] + ... \; \}.$$

We have new variables, $x = \frac{1}{2}\beta(f_c - f_d)A$, which measure the free energy difference between the confined and deconfined phases, and $\delta' = \delta \exp(-\beta\alpha_{cd}A)$, which is the Boltzmann weight for a fluctuating interface. For each configuration, the total Boltzmann weight is the product of the domain and interface weights. A confined domain k of length L_k has a domain factor $\exp(-xL_k)$, while a deconfined domain of the same length has a factor $\exp(xL_k)$. Summing the series to all orders, we obtain

$$Z = 2 \exp(-\beta(f_c + f_d)AL_z/2) \cosh[L_z\sqrt{x^2 + 3\delta'^2}]. \qquad (3.18)$$

Similarly, the diagrammatic terms for the expectation value of the Polyakov loop are

$Z\langle\Phi\rangle$ =

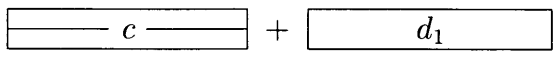

+ $\sum_i$ {

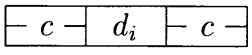

+

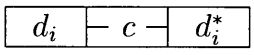

} + ... (3.19)

The center electric flux connecting the quark with its C-periodic partner is constricted

into a tube when it passes through a region of confined phase. Each term in the series corresponds to a configuration, whose contribution to $Z\langle\Phi\rangle$ is the Boltzmann weight for the configuration times the value of Φ in the configuration, integrating over all interface positions. Summing the series for $Z\langle\Phi\rangle$, we find that all terms with two or more interfaces cancel. In each deconfined domain, Φ can take with equal probability any of the values $\Phi^{(i)}, i \in \{1,2,3\}$ and, as $\sum_{i=1}^{3}\Phi^{(i)} = 0$, all these terms cancel. The same is true for each confined domain. Dividing out the partition function, the Polyakov loop expectation value is

$$\langle\Phi\rangle = \frac{\Phi_0 \exp(xL_z) + \Sigma_0 \exp(-(x+\beta\sigma)L_z)}{2\cosh[L_z\sqrt{x^2+3\delta'^2}]}. \tag{3.20}$$

There are two regions of qualitatively different behavior. If $f_d < f_c + \sigma/A$, i.e. it is energetically favorable to have deconfined phase as opposed to confined phase and a QCD string. From $\langle\Phi\rangle$, we extract the free energy of the test quark

$$F = -\frac{1}{\beta}\ln\Phi_0 + (\sqrt{x^2/\beta^2 + (3\delta^2/\beta^2)\exp(-2\beta\alpha_{cd}A)} - x/\beta)L_z, \tag{3.21}$$

which defines an effective "string tension"

$$\sigma' = \sqrt{x^2/\beta^2 + (3\delta^2/\beta^2)\exp(-2\beta\alpha_{cd}A)} - x/\beta. \tag{3.22}$$

Note that this effective string tension is independent of the actual QCD string tension σ. In particular, at the finite volume critical point, i.e. at $f_d = f_c$, we have

$$\sigma' = \frac{\sqrt{3}\delta}{\beta}\exp(-\beta\alpha_{cd}A). \tag{3.23}$$

For $f_d > f_c + \sigma/A$, on the other hand, where it is energetically favorable for the static quark to sit in confined phase, the quark free energy and the effective "string tension" are

$$F = -\frac{1}{\beta}\ln\Sigma_0 + (\sqrt{x^2/\beta^2 + (3\delta^2/\beta^2)\exp(-2\beta\alpha_{cd}A)} + x/\beta)L_z$$

$$\sigma' = \sigma + \sqrt{x^2/\beta^2 + (3\delta^2/\beta^2)\exp(-2\beta\alpha_{cd}A)} + x/\beta. \tag{3.24}$$

Note that now $x < 0$ and hence, as expected, σ' reduces to σ in the limit of $A \to \infty$. The finite volume behavior for $\langle\Phi\rangle$ we have calculated has the correct limiting behavior on both sides of the phase transition.

We have already said that the finite volume behavior of $\langle\Phi\rangle$ deep in the deconfined phase might be used to extract the deconfined-deconfined interface tension α_{dd}. It is also possible that finite volume behavior near the phase transition could be used to extract the confined-deconfined interface tension α_{cd}. We explore this possibility in Chapter 4.

3.5.2 Incomplete wetting

We now consider the alternative possibility at the phase transition, that the domain walls are incompletely wet. This does not seem to be realized in Nature, as numerical studies of $SU(3)$ pure gauge theory show that the domain walls appear to be completely wet. However, we can still apply the dilute interface gas expansion in this scenario. We still consider this case, simply to include all possibilities.

If incomplete wetting occurs at T_c, we can have both confined-deconfined and deconfined-deconfined domain walls. This gives us the most general possible interface expansion, where all numbers of interfaces are possible. Diagrammatically, the partition function takes the form

$Z =$ | c | $+$ | d_1 | $+$ | d_2 | d_3 |

$+$ | d_3 | d_2 | $+ \sum_i \{$ | c | d_i | c | $+$ | d_i | c | d_i^* | $\}$

$+ \sum_{i,j}$ | d_i | d_j | d_i^* | $+ \ldots$ (3.25)

The sum in the last term is restricted to $d_j \neq d_i, d_i^*$, i.e. the phases on either side of

an interface are distinct. In exact analagy to before, each diagram corresponds to a Boltzmann weight, which is determined by the number and type of interfaces and how much of the volume is in confined or deconfined phase. To calculate observables such as $\langle\Phi\rangle$, we include the value of the observable with the weight of each configuration. Note that if we eliminate the confined phase, the expansion simplifies to that deep in the deconfined phase, which we have already calculated. Similarly, if we exclude deconfined-deconfined interfaces, we reduce to the complete wetting expansion. These features should be apparent in the final result.

We calculate that

$$\begin{aligned}\langle\Phi\rangle &= \frac{\Phi_0 \exp((x-\gamma\exp(-\beta\alpha_{dd}A))L_z) + \Sigma_0\exp(-(x+\beta\sigma)L_z)}{2\cosh[L_z\sqrt{(x+\gamma\exp(-\beta\alpha_{dd}A))^2+3\delta^2\exp(-2\beta\alpha_{cd}A)}]} \\ &\times \exp(-\gamma\exp(-\beta\alpha_{dd}A)L_z). \end{aligned} \tag{3.26}$$

We see that if we eliminate the confined phase by taking the limits $\alpha_{cd}\to\infty, \sigma\to\infty$, this simplifies to the previous result found deep in the deconfined sector. Alternatively, if we eliminate deconfined-deconfined interfaces by letting $\alpha_{dd}\to\infty$, we simplify to the complete wetting result. This is the correct behavior. From $\langle\Phi\rangle$, we extract the free energy F. There are two possible scenarios. If $f_c + \sigma/A > f_d + (\gamma/\beta A)\exp(-\beta\alpha_{dd}A)$, i.e. the deconfined phase is energetically favorable, the free energy is

$$\begin{aligned} F &= -\frac{1}{\beta}\ln\Phi_0 \\ &+ \frac{1}{\beta}[2\gamma\exp(-\beta\alpha_{dd}A) - x + \sqrt{(x+\gamma\exp(-\beta\alpha_{dd}A))^2+3\delta^2\exp(-2\beta\alpha_{cd}A)}]L_z. \end{aligned} \tag{3.27}$$

On the other hand, if the confined phase is favored energetically, i.e. $f_c + \sigma/A < f_d + (\gamma/\beta A)\exp(-\beta\alpha_{dd}A)$, the free energy is given by

$$\begin{aligned} F &= -\frac{1}{\beta}\ln\Sigma_0 \\ &+ \frac{1}{\beta}[\beta\sigma + x + \gamma\exp(-\beta\alpha_{dd}A) + \sqrt{(x+\gamma\exp(-\beta\alpha_{dd}A))^2+3\delta^2\exp(-2\beta\alpha_{cd}A)}]L_z. \end{aligned} \tag{3.28}$$

In either case, we can define an effective "string tension" σ' as the free energy cost per unit length of the cylinder. As before, if incomplete wetting is realised at the phase transition, this finite volume dependence might be used to determine interface tensions numerically.

3.5.3 Alternative spatial boundary conditions

We have already said that if we choose all spatial directions to be C-periodic, we do not find any interesting behavior at temperatures greater than T_c. The cylinder will contain only deconfined phase d_1 with no interfaces. Close to the critical temperature, the situation changes. We have coexisting deconfined phase d_1 and confined phase c, both of which are compatible with C-periodicity. There are confined and deconfined domains, separated by confined-deconfined interfaces. Imposing C-periodic boundary conditions in all spatial directions eliminates deconfined phases d_2 and d_3, so the interface expansion is a subset of that for complete wetting. With only one deconfined phase, there cannot be wetting of deconfined-deconfined interfaces at T_c. We examine this situation with malice aforethought, as it turns out to be much easier to extract α_{cd} numerically in this scenario than from complete wetting. The diagrammatic expansion for the partition function is

$Z =$ 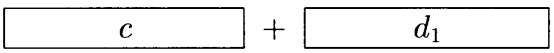 $+$

$+$ 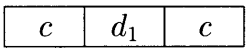 $+$ 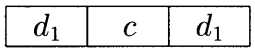 $+ \ldots$ (3.29)

Summing the series, we obtain

$$Z = 2\exp(-\beta(f_c + f_d)AL_z/2)\cosh(L_z\sqrt{x^2 + \delta'^2}). \tag{3.30}$$

As before, $x = \beta(f_c - f_d)A/2$ measures how far away we are from the finite volume critical point (where $f_c = f_d$) and $\delta' = \delta\exp(-\beta\alpha_{cd}A)$. To calculate $Z\langle\Phi\rangle$, as before, we include the value of the Polyakov loop with the Boltzmann weight for each possible

configuration. With C-periodicity in all spatial directions, the static test quark has a neighboring anti-quark in all directions. If the test quark is placed in a region of confined bulk phase, a QCD string connects the quark to the nearest anti-quark, which will be in the x- or y-direction. Including the additional energy cost of the QCD string, we calculate

$$\begin{aligned}\langle\Phi\rangle &= \Big\{[\frac{\Phi_0+\Sigma_0'}{2}+\frac{x(\Phi_0-\Sigma_0')}{2\sqrt{x^2+\delta'^2}}]\exp(L_z\sqrt{x^2+\delta'^2})+ \\ &\quad [\frac{\Phi_0+\Sigma_0'}{2}-\frac{x(\Phi_0-\Sigma_0')}{2\sqrt{x^2+\delta'^2}}]\exp(-L_z\sqrt{x^2+\delta'^2})\Big\}/2\cosh(L_z\sqrt{x^2+\delta'^2}),\end{aligned} \tag{3.31}$$

where $\Sigma_0' = \Sigma_0\exp(-\beta\sigma L_\perp), L_\perp = \min(L_x, L_y)$. We test this new result in two limits. If we are on the deconfined side of the phase transition, then $f_d < f_c$ and we find that, as the volume grows large, $\langle\Phi\rangle = \Phi_0$. This is as we expect — a domain wall costs more and more energy, so the whole volume is filled with deconfined phase d_1 and the quark energy is independent of the volume size. If we are on the confined side of the phase transition with $f_d > f_c$, as the volume becomes large, $\langle\Phi\rangle = \Sigma_0\exp(-\beta\sigma L_\perp)$ and $F = (-1/\beta)\ln\Sigma_0 + \sigma L_\perp$. The entire volume is filled with confined phase and the quark is connected to the nearest anti-quark by a QCD string. This analytical result shows how the finite volume behavior of the Polyakov loop changes across the deconfinement phase transition with C-periodicity in all directions. We can also use this expression to extract the confined-deconfined interface tension α_{cd} from numerical simulations.

3.6 Summary

In conclusion, we have found a paradoxical mechanism for confinement that works even deep in the deconfined phase, provided the Universe is a cylinder and has specific boundary conditions. Our calculation relates the presence of interfaces to the free energy of a static quark and thus shows that deconfined-deconfined interfaces have physically observable consequences. Even though an experimentalist cannot choose

the boundary conditions of the Universe, a lattice field theorist, performing a numerical simulation of the gluon system, can. In fact, one can use our results to extract the string tension σ, as well as the interface tensions α_{cd} and α_{dd}, from simple lattice measurements of a single Polyakov loop in cylinders of various A and L_z, which are then fitted to the appropriate analytic behavior. This may turn out to be technically easier than applying standard methods.

We have considered the confined and deconfined phases only of ordinary $SU(3)$ pure gauge theory. As discussed in Chapter 2, there are similar phases at non-zero temperature in $\mathcal{N} = 1$ supersymmetric $SU(3)$ Yang-Mills theory. The same finite volume formulae for $\langle\Phi\rangle$ in cylindrical geometries are valid in this theory, e.g. a static test quark is confined even in the deconfined sector, due to multiple deconfined domains. The supersymmetric theory has six phases in total, three confined and three deconfined, which changes some numerical factors, but the general form of the volume dependence is the same. Analogous finite volume formulae also hold for the expectation value of the gluino condensate $\chi = \langle\Psi^a\Psi_a\rangle$.

We have shown that we can have confinement in the deconfined phase. In Chapter 2, we showed in the supersymmetric pure gauge theory that QCD strings can end on domain walls. This suggests that perhaps quarks can be screened from one another by domain walls that separate them. Is the converse possible, that we can have deconfinement in the confined phase? We consider a domain wall in the supersymmetric theory, separating two distinct confined phases. On one side of the wall is a quark, on the other an anti-quark. If the QCD string emanating from the quark can end on the domain wall, the quark's free energy is independent of where the anti-quark is and we could say that the quark is deconfined. However, this is only possible if the domain wall is of infinite extent and can transport the color flux to infinity at a finite energy cost. If the domain wall is finite, the color flux must emerge somewhere and end on the anti-quark. We could consider the quark bound to an infinite domain wall as deconfined, but this seems very artificial. A quark bound to a finite domain wall is still connected to an anti-quark and is confined. The converse is not true — we do not have deconfinement in the confined phase.

Chapter 4

Numerical study of confinement in deconfined phase

4.1 Motivation for numerical study

In Chapter 3, we considered the behavior of $SU(3)$ Yang-Mills theory at non-zero temperature in finite volumes. We calculated the free energy of a single static test quark in cylinders, using C-periodic boundary conditions in the long direction which made it possible for a single quark to be in the volume. At low temperature, the quark sits in a gluonic background of confined phase and is connected via a QCD string to its partner anti-quark on the other side of the C-periodic boundary. In the confined phase, the quark free energy is proportional to the cylinder length. As expected, the free energy diverges as quark and anti-quark are infinitely separated, the quark is confined. At high temperature, the volume is filled with many domains of deconfined phase, which are separated by domain walls. Although sitting in deconfined phase, the free energy of a quark in this volume is still proportional to the cylinder length. This is the unusual confinement in the deconfined phase. The quark free energy diverges, even though there is no QCD string present.

We are interested to see if this unexpected confinement in the deconfined phase can be observed in a numerical study. The dilute interface gas expansion assumes that the cylinder is filled with domains, separated by domain walls which are transverse

to the longitudinal direction. The calculation also assumes that the interfaces do not interact. Domain walls are observed in numerical simulations of the pure gauge theory and it is certainly true that if we go to arbitrarily large volumes, the domain wall structure will appear in the cylinder. Also, as both the confined and deconfined phases are massive, we expect interface interactions to fall off exponentially, so the dilute approximation should be valid in large volumes. However, the signal for the confinement is that the Polyakov loop expectation value should fall off exponentially with the length of the cylinder. We can only observe a numerical signal in moderately sized cylinders and it is not at all clear that the assumptions hold in these relatively small volumes. If it is possible to observe this behavior numerically, this would be a new technique to extract the interface tension of domain walls.

4.2 Effective theory for $SU(3)$ gauge theory

Numerical simulations of gauge theories are computationally intensive. We wish to measure an exponentially small number, which will require very large statistics. It would require a very large amount of work to see whether or not the unusual confinement can be observed in the full gauge theory. Our main interest is to see if this phenomenon is observable at all. In our analytical calculation, we needed to know if we were in the confined or deconfined sector of the theory. We did not need all the microscopic details of the Yang-Mills theory. We examine a simpler model, which is an effective theory for confinement and deconfinement in the full gauge theory. If we can observe unusual confinement in the simpler model, this tells us that our analytical calculation was valid and that the same phenomenon could, with enough work, be detected in Yang-Mills theory.

We consider the 3-dimensional 3-state Potts model, which is a lattice model of spins at lattice sites. It is an effective theory for non-zero temperature $SU(3)$ Yang-Mills theory. We explain why it is an effective theory and show how we can observe the unusual confinement even in relatively small volumes using highly efficient numerical techniques. In the 3-dimensional 3-state Potts model, there are spins Φ_x at lattice

sites x which can take one of three values $\Phi_x \in \mathbf{Z}(3) = \{\exp(2\pi in/3), n = 1, 2, 3\}$. The action is

$$S[\Phi] = -\kappa \sum_{\langle xy \rangle} \delta_{\Phi_x, \Phi_y}, \tag{4.1}$$

where the sum is over nearest neighboring spins at x and y. Neighboring spins with the same value contribute $-\kappa$ to the action, those with values different from each other contribute zero. The action is minimized by all spins having the same value. If we globally rotate all spins to $\Phi'_x = \Phi_x z, z \in \mathbf{Z}(3)$, the action is unchanged. Neighboring spins with the same value are still the same, those with differing values are still different. This global symmetry is exactly analogous to the $\mathbf{Z}(3)_c$ center symmetry of the Yang-Mills theory. Numerical work shows that this model has a first order phase transition at a non-zero coupling κ_c [8]. For $\kappa < \kappa_c$, the system is in a disordered phase, where $\langle \Phi \rangle$ is zero and the global $\mathbf{Z}(3)$ symmetry is intact. For $\kappa > \kappa_c$, there are three ordered phases, where $\langle \Phi \rangle = \Phi^{(n)} = \Phi_0 \exp(2\pi in/3), n \in \{1, 2, 3\}$ and the global $\mathbf{Z}(3)$ symmetry is broken. The disordered phase is exactly analogous to the confined phase of the Yang-Mills theory, while the three ordered phases correspond to the three deconfined phases. Because of this shared global symmetry and phase structure, the Potts model is an effective theory to describe the deconfinement phase transition.

We look at the behavior of Potts spins in cylindrical volumes of dimension $L_x \times L_y \times L_z$, where $L_z \gg L_x, L_y$. We impose ordinary periodicity in the x- and y-directions and C-periodicity in the z-direction. We can again apply C-periodicity because charge conjugation is a symmetry of the Potts action. Using the dilute gas of interfaces, we calculate that the average spin $\langle \Phi \rangle$ in this volume deep in the ordered (deconfined) regime is

$$\langle \Phi \rangle = \Phi_0 \exp(-3\gamma \exp(-\kappa \alpha_{dd} A) L_z). \tag{4.2}$$

Now we have an interface tension α_{dd} for an interface between two ordered phases and γ accounts for the fluctuation of these non-rigid domain walls. Previously, the Polyakov loop fell off exponentially with the cylinder length, signalling confinement.

This now becomes the exponential fall off of the average spin. Similarly, we calculate the average spin near the phase transition with the interface expansion for the different cases of complete wetting, incomplete wetting and C-periodicity in all spatial directions. We find that the average spin has the same volume dependence as the Polyakov loop expectation value. Near κ_c, $\langle\Phi\rangle$ depends on α_{cd}, the energy cost of an interface between an ordered and a disordered phase. The analytical results have an identical form, translating deconfined and confined bulk phases into ordered and disordered bulk phases. However, the numerical values of quantities such as interface tensions will be not be the same in the effective theory as they are in the full gauge theory.

4.3 Monte Carlo numerical techniques

4.3.1 Importance sampling

We can define a model by an action S which is a functional of some number of degrees of freedom. For example, the QCD action is a functional of quark and gluon fields. We construct the partition function of the theory Z by functionally integrating over all the degrees of freedom. As every observable quantity can be obtained by including source terms in the action and taking functional derivatives of the source dependent Z, the partition function contains complete information about the model. However, it is not possible in general to compute observables analytically. Instead, we use numerical methods to estimate observables for a given model.

In the following, we use the 3-dimensional 3-state Potts model as a specific example of numerical techniques that are very generally applicable. Given the action $S[\Phi]$ of this model as above, the partition function is

$$Z = \int \prod_x [D\Phi_x] \ \exp(-S[\Phi]) = \int [D\Phi] \ \exp(-S[\Phi]), \tag{4.3}$$

where we integrate over all spin values Φ_x at every position x. A configuration Φ of the system is described by each spin having some value. The partition function is the

integral over all configurations. An observable such as the average spin is calculated as

$$\langle \Phi \rangle = \frac{1}{Z} \int \prod_x [D\Phi_x] \, \frac{1}{V} \sum_x \Phi_x \exp(-S[\Phi]), \tag{4.4}$$

where V is the volume. If we restrict ourselves to finite volumes, this becomes a finite dimensional functional integral, which we still cannot analytically compute. We estimate this integral numerically using Monte Carlo integration. We are given a probability density, in this case the Boltzmann weight. The configurations of the system with the largest probability density are those which make the most significant contribution to the observable. Configurations with very small weight make very small contributions to the observable. If we sample the entire configuration space using the probability density and determine which configurations are "important", we can estimate the observable from a reasonably small number of configurations. For example, if we consider the 3-state Potts model in a cube of dimension $5 \times 5 \times 5$, there are $3^{125} \approx 4 \times 10^{59}$ possible configurations. However, we only require a relatively small number of configurations to estimate observables. From the entire ensemble of configurations, we sample those which are most important, based on energy and entropy considerations. Using importance sampling to explore the configuration space and to estimate observables from a relatively small number of configurations is Monte Carlo integration [46].

4.3.2 Markov chains and detailed balance

Using the probability density, we generate a sequence of configurations $\Phi^{(i)}$, starting from some initial randomly chosen configuration $\Phi^{(1)}$. Each configuration in this sequence is generated by some probabilistic method only from its immediate predecessor. However, it is not statistically independent of all other previous configurations. This sequence is a Markov chain. If we terminate the chain with n configurations, we estimate, for example, the average spin as

$$\langle \Phi \rangle \approx \frac{1}{n} \sum_{i=1}^{n} \langle \Phi[\Phi^{(i)}] \rangle = \frac{1}{n} \sum_{i=1}^{n} (\frac{1}{V} \sum_x \Phi_x^{(i)}), \tag{4.5}$$

where $\Phi_x^{(i)}$ is the value of the spin at x in configuration $\Phi^{(i)}$. We denote by $P[\Phi, \Phi']$ the transition probability that, given a configuration Φ in the Markov chain, the next configuration we generate is Φ'. The choice of $P[\Phi, \Phi']$ is an algorithm and, as a probability, has certain constraints, i.e.

$$P[\Phi, \Phi'] \geq 0 \quad \forall\ \Phi, \Phi', \qquad \int [D\Phi]\ P[\Phi, \Phi'] = 1. \tag{4.6}$$

The probability of generating any configuration from another must be non-negative and, given a configuration Φ, we generate some new configuration with probability 1. As the Markov chain grows longer, each configuration should appear with the correct equilibrium distribution. One property we want to have is that, if we have an ensemble of configurations with the correct equilibrium probability density, the Markov process leaves the ensemble in equilibrium. In the case where the equilibrium density is the Boltzmann weight, this is

$$\int [D\Phi]\ \exp(-S[\Phi])\ P[\Phi, \Phi'] = \exp(-S[\Phi']). \tag{4.7}$$

Configuration Φ appears in the ensemble with weight $\exp(-S[\Phi])$. After we have applied the Markov process to each configuration to generate a new ensemble, Φ' appears with weight $\exp(-S[\Phi'])$.

We can guarantee that the Markov process leaves the equilibrium distribution unchanged by making it satisfy a condition known as detailed balance. For the Boltzmann distribution, this is

$$\exp(-S[\Phi])\ P[\Phi, \Phi'] = \exp(-S[\Phi'])\ P[\Phi', \Phi]. \tag{4.8}$$

The weight of configuration Φ times the probability of transforming Φ into Φ' equals the weight of configuration Φ' times the probability of transforming Φ' into Φ. Integrating over Φ, we obtain

$$\int [D\Phi]\ \exp(-S[\Phi])\ P[\Phi, \Phi'] = \exp(-S[\Phi'])(\int [D\Phi]\ P[\Phi', \Phi]) = \exp(-S[\Phi']), \tag{4.9}$$

which is the equilibrium condition for the Markov process.

4.3.3 Metropolis algorithm and critical slowing down

We are free to choose any set of probabilities $P[\Phi, \Phi']$ which satisfy the required conditions. One straightforward choice is the Metropolis algorithm [47]. We pick a single position x in configuration Φ and choose at random a new value for the spin Φ_x, generating a new configuration Φ'. The probability of accepting the new spin value is the probability $P[\Phi, \Phi']$, which is determined by the values of the action of the two configurations,

$$\begin{aligned} S[\Phi'] < S[\Phi] &\implies P[\Phi, \Phi'] = 1, \\ S[\Phi'] > S[\Phi] &\implies P[\Phi, \Phi] = \exp(-\Delta S), \Delta S = S[\Phi'] - S[\Phi]. \end{aligned} \tag{4.10}$$

If the new choice lowers the action, we accept this with probability 1. If the new choice increases the action, we accept this with a probability determined by the change in the action. Note that, if $P[\Phi, \Phi'] = \exp(-\Delta S)$, then $P[\Phi', \Phi] = 1$, and vice versa. Taking the case that $S[\Phi'] > S[\Phi]$, we check that this algorithm satisfies detailed balance, as

$$\begin{aligned} P[\Phi, \Phi'] \ \exp(-S[\Phi]) &= \exp(-\Delta S) \ \exp(-S[\Phi]) = \exp(-S[\Phi'] + S[\Phi] - S[\Phi]) \\ &= \exp(-S[\Phi']) \\ P[\Phi', \Phi] \ \exp(-S[\Phi']) &= \exp(-S[\Phi']). \end{aligned} \tag{4.11}$$

In the alternative case, where $S[\Phi'] < S[\Phi]$, we have $P[\Phi, \Phi'] = 1$ and $P[\Phi', \Phi] = \exp(S[\Phi'] - S[\Phi])$. It is straightforward to show that detailed balance is again satisfied.

The computational advantage of the Metropolis algorithm is that the proposed change to the configuration is local and so the probability of accepting or rejecting the new configuration can be calculated extremely quickly. No time is wasted on proposing large scale changes to the configuration which are typically rejected. However, the locality of the Metropolis algorithm is also disadvantageous. Each pair of

consecutive configurations in the Markov chain differ by at most the value of the spin at one point. It takes very many iterations to generate independent configurations, i.e. for the system to lose "memory" of where it came from. We now make this idea more precise.

In the Markov chain, we calculate an observable, say the average spin, in each configuration, $\Phi^{(i)}, i = 1, 2, ..., n$. The autocorrelation between configurations of the average spin is

$$\begin{aligned} C_\Phi(t) &= \langle \Phi^{(1)} \Phi^{(t+1)} \rangle - \langle \Phi \rangle^2, \\ \langle \Phi^{(1)} \Phi^{(t+1)} \rangle &= \frac{1}{n-t} \sum_{i=1}^{n-t} \left(\frac{1}{V^2} \sum_{x,y} \Phi_x^{(i)} \Phi_y^{(i+t)} \right). \end{aligned} \tag{4.12}$$

This correlation decays as $C_\Phi(t) \propto \exp(-t/\tau_{exp})$, where τ_{exp} is the exponential autocorrelation time. This tells us about the correlations in the Markov chain which the algorithm is taking longest to destroy, which is independent of which observable we consider. More importantly, we calculate the integrated autocorrelation time

$$\tau_{int,\Phi} = \frac{1}{2} + \sum_{t=1}^{t=n-1} C_\Phi(t)/C_\Phi(0), \tag{4.13}$$

which integrates over all correlations in the Markov chain. In estimating the statistical error in an observable from n configurations, the true error is

$$\Delta\Phi = \sqrt{\frac{2\tau_{int,\Phi}}{n-1}} \quad \sqrt{\langle \Phi^2 \rangle - \langle \Phi \rangle^2}. \tag{4.14}$$

This is bigger than the naive statistical error by a factor $\sqrt{2\tau_{int,\Phi}}$ [48]. The number of configurations required to make the statistical error small is determined by $\tau_{int,\Phi}$, which is determined by the algorithm. Near a phase transition, the system undergoes changes at large scales and the correlation length ξ becomes large. Close to criticality, the exponential autocorrelation time behaves as $\tau_{exp} \approx a\xi^z$, where z is the dynamical critical exponent. Local algorithms, such as the Metropolis alogorithm, are unable to reflect the large-scale physics by making large-scale changes to configurations and they have a dynamical exponent $z \approx 2$. For critical behavior where ξ is of the order

of 100, we have τ_{exp} on the order of 10 000. This phenomenon of the algorithm taking longer and longer to generate statistically independent configurations is known as critical slowing down. Because the number of configurations required increases with roughly the square of the correlation length, it is not possible in practice to observe large scale critical behavior with local algorithms. When critical slowing down occurs, an algorithm is said to be inefficient.

4.3.4 Cluster algorithms

There are alternative algorithms for which the critical slowing down is not as severe or possibly even eliminated. One such class of algorithms is cluster algorithms [49]. These algorithms make large scale non-local changes to configurations. However, they do not have the problem of suggesting large scale changes which are typically rejected. A configuration is decomposed into several connected clusters and the average cluster size is on the order of the correlation length. Clusters consist of, for example, spins at different positions, which are bonded or frozen together i.e. if one spin in the cluster is changed, all of them want to be changed. Configuration updates are achieved by making changes to each cluster. If the system undergoes critical behavior, the large correlation length is reflected in the cluster sizes. In some cases, cluster algorithms have a dynamical exponent $z \approx 0$, practically eliminating the critical slowing down. In the following Section, we describe in detail a cluster algorithm for the 3-state Potts model.

4.4 Cluster algorithm for the Potts model

4.4.1 Cluster building rules

We describe a cluster algorithm for the 3-dimensional 3-state Potts model, which is the effective theory for $SU(3)$ pure gauge theory at non-zero temperature. A configuration consists of some value for the spin Φ_x at each position x. We consider volumes of dimension $L_x \times L_y \times L_z$, where $L_z \gg L_x, L_y$. We pick a spin at random

from the cylinder as the first element of a cluster. Usually, this spin will get a new value. Next, we examine all pairs of the original spin and its nearest neighbors. If both spins in a pair have the same value, they make a contribution $-\kappa$ to the action, if they are different, they make a zero contribution. If both spins are alike and we change one, the action is increased by κ. Neighboring spins which are the same would like to stay the same, so we "freeze" them together with probability $P = 1 - \exp(-\Delta S) = 1 - \exp(-\kappa)$. Freezing together means including neighboring spins in the same cluster. Note that at very large couplings, $\kappa \to \infty$ and $P \to 1$, i.e. neighboring same-value spins always want to be frozen together. At very small couplings, $\kappa \to 0$ and $P \to 0$, i.e. neighboring spins want to fluctuate independently. We consider each nearest neighbor of the original spin — if it has the same spin value, we include it in the cluster with probability P, if it has a different value, we don't include it in the cluster. We continue to grow the cluster until all nearest neighbors of all spins in the cluster have been examined. Once the cluster is fully grown, we start a new cluster on some spin which is not included. We continue to grow clusters until every spin in the configuration is included in one and only one cluster.

In each cluster, all the spins have the same value. We update the configuration by "flipping" a cluster, i.e. all the spins in a cluster are given a new randomly chosen value. Usually, it is possible to flip a cluster to any new value, so we make large scale changes to the system which are typically accepted, obviating the difficulty of critical slowing down. As the system is decomposed into many clusters, this is a multicluster algorithm.

4.4.2 Detailed balance

We show detailed balance is satisfied by looking at configurations $\Phi^{(i)}$ of only two neighboring spins, Φ_1 and Φ_2. We need to show detailed balance is satisfied between all possible configurations Φ and Φ', i.e. $\exp(-S[\Phi])\ P[\Phi, \Phi'] = \exp(-S[\Phi'])\ P[\Phi', \Phi]$. Using the values in Table 4-1, we consider all the possible cases separately.

Table 4.1: Boltzmann weights and freezing/non-freezing probabilities for a pair of neighboring spins

Spin values	Boltzmann weight	P_{frozen}	$P_{unfrozen}$
same	$\exp(\kappa)$	$1-\exp(-\kappa)$	$\exp(-\kappa)$
different	1	0	1

1. $\Phi : \Phi_1 = \Phi_2, \quad \Phi' : \Phi'_1 = \Phi'_2$

   Both of these configurations weight $\exp(\kappa)$ and $P[\Phi, \Phi'] = P[\Phi', \Phi] = 1 - \exp(-\kappa)$ — we can only generate one configuration from the other by freezing the spins together. Detailed balance is satisfied.

2. $\Phi : \Phi_1 = \Phi_2, \quad \Phi' : \Phi'_1 \neq \Phi'_2$

   Configuration Φ has weight $\exp(\kappa)$ and Φ' has weight 1. We can only generate one configuration from the other if the spins are not frozen together, i.e. $P[\Phi, \Phi'] = \exp(-\kappa)$ and $P[\Phi', \Phi] = 1$. Detailed balance is satisfied.

3. $\Phi : \Phi_1 \neq \Phi_2, \quad \Phi' : \Phi'_1 \neq \Phi'_2$

   Both configurations have weight 1 and we can only generate one configuration from the other if the spins are not frozen together, i.e. $P[\Phi, \Phi'] = P[\Phi', \Phi] = 1$, which is in fact the only choice. Detailed balance is satisfied.

4.4.3 Improved estimator

The average spin is

$$\langle \Phi \rangle = \frac{1}{V} \langle \sum_x \Phi_x \rangle = \frac{1}{V} \langle \sum_C \sum_{x \in C} \Phi_x \rangle = \frac{1}{V} \langle \sum_C |C| \langle\langle \Phi \rangle\rangle_C \rangle, \tag{4.15}$$

i.e. the average spin is the average over all spins in the volume divided by the total volume V. We can sum all the spins in two steps — first we sum over all the spins contained in a single cluster C of volume $|C|$, then we sum over all the clusters. We then find the average spin in each cluster $\langle\langle \Phi \rangle\rangle_C$ by allowing the spins in the cluster to assume all possible values. In a finite volume where all spatial directions are periodic,

the spins in each cluster can assume all values $\Phi^{(n)} = \exp(2\pi i n/3), n \in \{1,2,3\}$ with equal probability and, as $\sum_n \Phi^{(n)} = 0$, the average spin in each cluster $\langle\langle\Phi\rangle\rangle_C$ is zero, which tells us that the average spin vanishes. This is simply reproducing what we have previously said, that we cannot have a single quark in a periodic volume, so the Polyakov loop expectation value is zero.

Our analytic calculations are valid for cylinders which are C-periodic in the long direction and periodic in the short directions. In such volumes, there are two types of clusters: those which wrap around the C-periodic direction an odd number of times and those which wrap around an even number of times (which includes those which do not wrap around at all). We call these wrapping and non-wrapping clusters respectively. A wrapping cluster can only satisfy C-periodicity if it contains spins with real value 1. We cannot flip these spins to a new complex value, as that would break the C-periodicity. The average spin in each wrapping cluster is $\langle\langle\Phi\rangle\rangle_C = 1$. The spins in a non-wrapping cluster take any value with equal probability and still satisfy C-periodicity. The average spin in each non-wrapping cluster is $\langle\langle\Phi\rangle\rangle_C = 0$.

In each iteration of the multicluster algorithm, we decompose the entire volume into clusters, measuring the total volume of wrapping clusters $|C|_{WC}$. We then flip the non-wrapping clusters' spins to randomly chosen new values to generate a new configuration. The total average spin is determined by the average of $|C|_{WC}$,

$$\langle\Phi\rangle = \frac{1}{V}\langle\sum_{WC}|C|_{WC}\rangle. \tag{4.16}$$

Every configuration has $|C|_{WC} \geq 0$, so we only make non-negative contributions to our estimate of $\langle\Phi\rangle$. This is an improved estimator, as there is no cancellation between positive and negative contributions. The average spin falls off exponentially with the cylinder length, so the numerical signal is very small. With many positive and negative contributions, it would be very difficult to measure such a small signal. It is essential that we use an improved estimator, which we commonly have with cluster algorithms.

Instead of decomposing the entire configuration into clusters in each iteration

(a multicluster algorithm), we can build just one cluster in each iteration. This is a single cluster algorithm. Instead of estimating the average spin by summing the average spin of all clusters, we only determine the average spin in one single cluster C. The probability of choosing this cluster from all of them is proportional to its size, i.e. $P_C = |C|/V$. The average spin is then

$$\langle \Phi \rangle = \frac{1}{V} \langle \frac{|C| \langle\langle \Phi \rangle\rangle_C}{P_C} \rangle = \langle \langle\langle \Phi \rangle\rangle_C \rangle = P_{wrap}, \tag{4.17}$$

the sum over all cluster averages is replaced by one cluster average divided by the probability P_C of choosing that cluster. The average spin in the entire volume equals the average spin in the single cluster that we build, which equals the probability P_{wrap} that the single cluster is a wrapping cluster. To estimate this probability numerically, we build a single cluster — if it is wrapping, we count a 1, if it is non-wrapping, we count a 0. We repeat this procedure until we can accurately estimate the wrapping probability. Again, this is an improved estimator because we only add non-negative numbers in making our estimate of P_{wrap}. For very long and thin cylinders, P_{wrap} is very small and such a small signal would be very difficult to detect if we had positive and negative contributions to our estimator with lots of cancellation. The signal is small but the improved estimator does the best possible job of numerically estimating the probability.

4.5 Numerical results

4.5.1 Deconfined phase

We first consider the case deep in the ordered (deconfined) phase of the theory, where we expect $\langle \Phi \rangle$ to decrease exponentially with the cylinder length, which is the signal in this effective model for the unusual confinement. Here, we use the single cluster algorithm to estimate $\langle \Phi \rangle$, as it is faster than the multicluster algorithm. Previous work has determined that the phase transition occurs at $\kappa_c = 0.550565(10)$ [8]. The ordered regime is $\kappa > \kappa_c$. If we go too far away from κ_c, the energy cost of even one

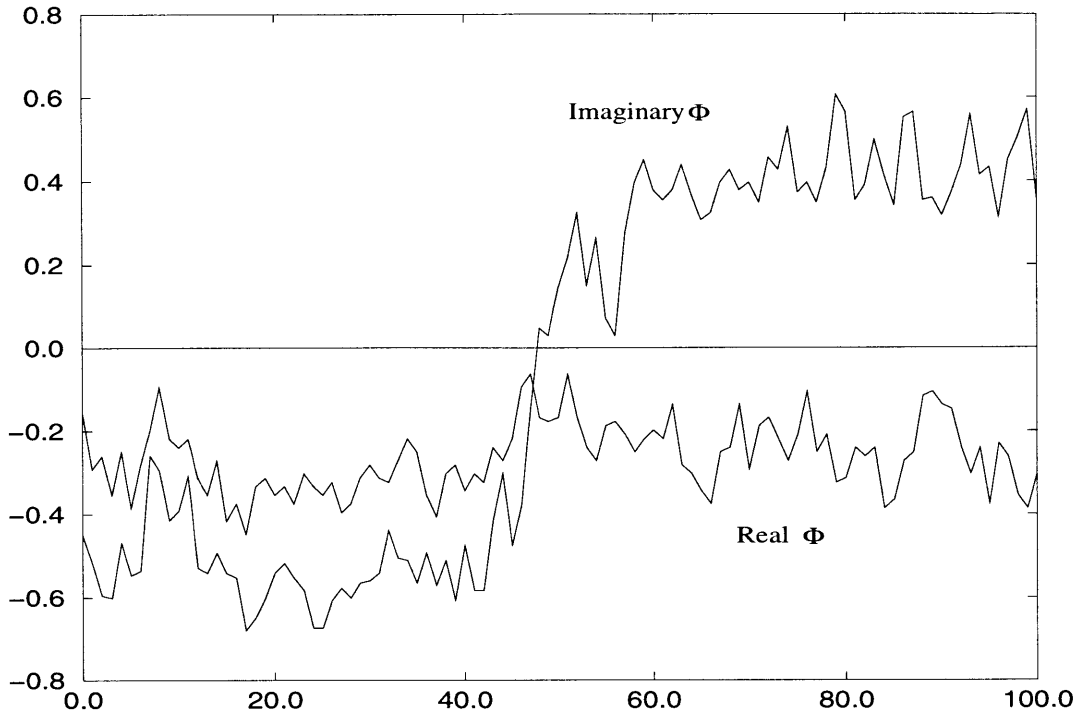

Figure 4-1: *The spins Φ_x are averaged over the transverse plane located at longitudinal coordinate z. The plot is of the real and imaginary parts of the planar average of the spin versus z. There is one interface, separating two of the ordered bulk phases.*

interface will be very large, an interface will practically never appear in the volume and our analytical calculation will not apply. We work in a region $\kappa_c < \kappa < 1.005\kappa_c$, where typically there are interfaces in the cylinder. The volumes we examine are of transverse dimension $L_x = L_y = 12, 13, 14$ and L_z in the range 80 to 120. In a typical simulation, we perform 10 000 iterations to reach equilibrium and 1 000 000 iterations which we use to estimate P_{wrap}. We find that the integrated autocorrelation time $\tau_{int,\Phi}$ is on the order of 10-20 iterations, so we see that the cluster algorithm quickly decorrelates configurations. This gives a true statistical error in $\langle\Phi\rangle$ on the order of 5% or less.

In Figure 4-1, we show a typical numerical configuration of a volume of dimension $12 \times 12 \times 100$ at a coupling $\kappa = 1.003\kappa_c$. To see if the domain wall structure appears in the cylinder, we need to determine which ordered phase occupies which part of the volume. To do this, we average Φ_x over each plane transverse to the long direction. In Figure 4-1, we plot the real and imaginary parts of this average. There are other

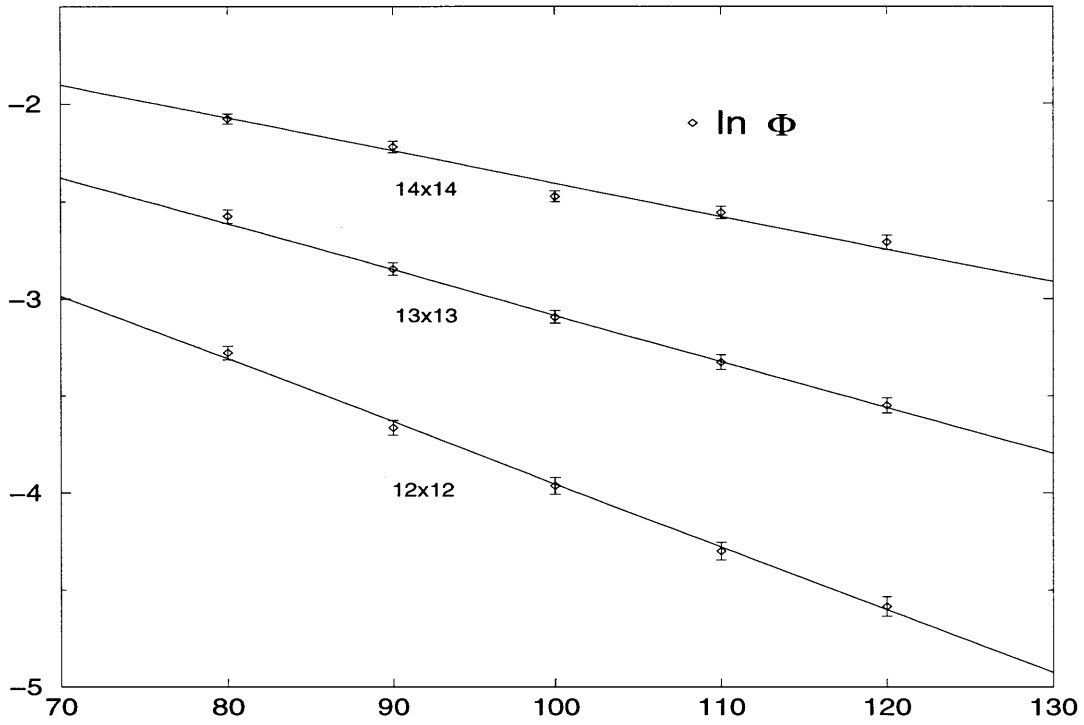

Figure 4-2: *A plot of* $\ln\langle\Phi\rangle$ *versus* L_z*, the cylinder length. The lines are the fit to the predicted analytical behavior of* $\ln\langle\Phi\rangle$ *in the ordered phase regime.*

methods of determining the phases, e.g. we say that each tranverse plane has the value of the spin $\Phi^{(n)} = \exp(2\pi in/3), n \in \{1,2,3\}$ which occurs most frequently in it. The particular configuration we have plotted has one interface with bulk ordered phase $\Phi = (-1 - i\sqrt{3})\Phi_0/2$ on the left hand side and ordered phase $\Phi = (-1 + i\sqrt{3})\Phi_0/2$ on the right.

At many different values of κ, we measure $\langle\Phi\rangle$ in cylinders of various lengths and cross-sectional areas. In Figure 4-2, we have plotted the numerical results for $\ln\langle\Phi\rangle$ in these various cylinders at a particular coupling, here $\kappa = 1.0035\kappa_c$. We see clearly that $\ln\langle\Phi\rangle$ falls linearly with L_z, i.e. the average spin falls off exponentially with the length of the cylinder. This is the effective theory analog for confinement in the deconfined phase. The single cluster algorithm and associated improved estimator are able to detect this extremely small signal. We see that our analytical calculation, which is certainly true for arbitrarily large volumes, also holds for volumes of moderate size. We fit the numerical data to the analytical formula. Each line in Figure 4-2 corresponds to a cylinder with a fixed area, i.e. $12 \times 12, 13 \times 13$ and 14×14. All

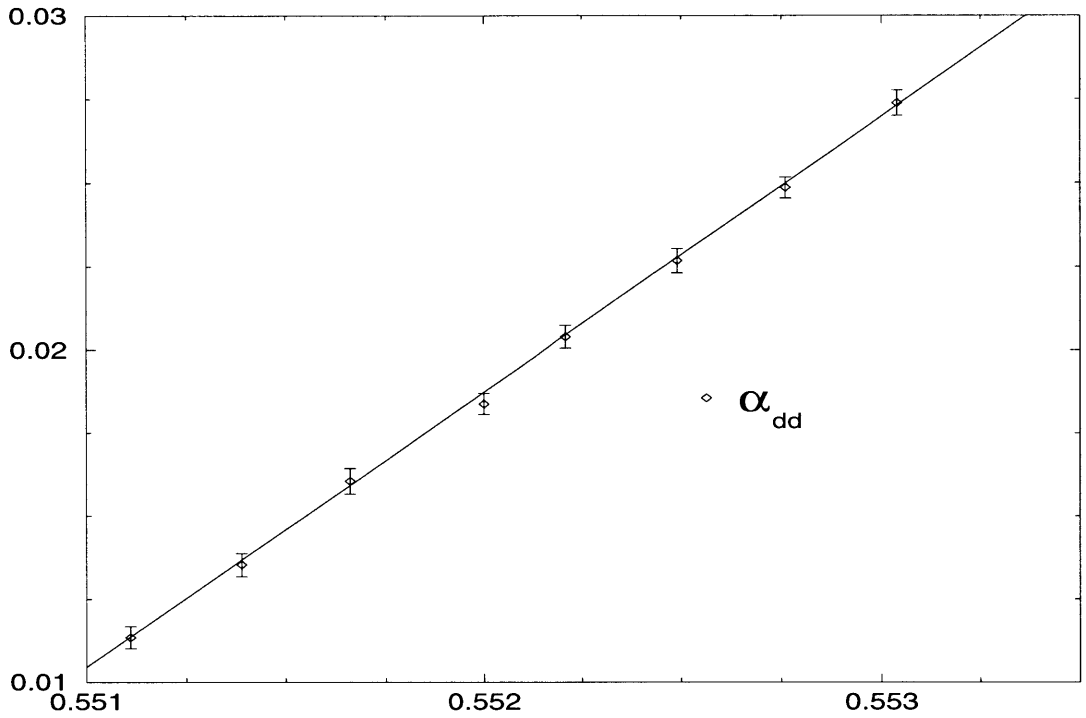

Figure 4-3: *The ordered-ordered interface tension α_{dd} as a function of κ. The fit is a straight line.*

three lines are obtained from one fit, which gives the numerical value of the ordered-ordered interface tension $\alpha_{dd}(\kappa)$ with χ^2 per degree of freedom ~ 0.7. We take this to be an indication of a good fit. We have performed simulations at many values of κ, including one previously examined in the literature, allowing us to make a direct comparison of the interface tension. At $\kappa = 0.552$, translating into our notation, a value of $\alpha_{dd} = 0.01796(14)$ has previously been determined [50]. Using our technique, we find $\alpha_{dd} = 0.01838(42)$, which is in agreement within error bars. This consistency check tells us that the interface tensions we extract are accurate.

At each value of κ, we extract $\alpha_{dd}(\kappa)$ from the fit of the numerical data to the predicted analytical form. In Figure 4-3, we plot all the values we have determined for α_{dd} as a function of κ. The data fits very well to a straight line, with χ^2/d.o.f ~ 0.2. The fit is

$$\alpha_{dd}(\kappa) = -4.54(4) + 8.26(8)\kappa, \tag{4.18}$$

where the uncertainties in the final digits are paranthesized. The uncertainties appear rather large, but this is actually because the parameters are highly correlated with

one another. At the critical point, it is expected that $\alpha_{dd}(\kappa_c) = 2\alpha_{cd}$ due to complete wetting. It is tempting to extrapolate our linear fit to the critical point to estimate the ordered-disordered interface tension α_{cd}. However, our configurations do not contain disordered phase and our numerical data cannot know anything about the energy cost of an ordered-disordered domain wall. We cannot extrapolate the fit deep in the ordered phase to the critical point.

4.5.2 Critical region

We now examine the Potts model near the phase transition, imposing C-periodicity only in the z-direction. In this case, we hope to find complete wetting of domain walls. If we observe the predicted finite volume behavior of $\langle\Phi\rangle$, we can extract the ordered-disordered interface tension α_{cd}. However, we are not able to see this behavior in numerical simulations. As we approach the critical coupling from above, the volume contains more and more disordered phase. Using the single cluster algorithm, P_{wrap}, the probability of building a single wrapping cluster of spins with value 1, becomes very small. Even after millions of iterations, we cannot reliably estimate the wrapping probability near κ_c. The multicluster algorithm is also not able to measure reliably the average number of spins in wrapping clusters. Far from criticality, the ordered domains in typical configurations are quite easily distinguished. Near criticality, it becomes much more difficult to identify domains, as we have three ordered and one disordered phase. Using the planar average of the spins to define domains shows large fluctuations, especially in what appear to be disordered domains. If complete wetting occurs, ordered domains should be separated from one another by films of disordered phase. Unable to confidently identify the disordered phase, we cannot confirm that complete wetting occurs at the phase transition. We also cannot numerically determine α_{cd} in this case.

We now consider the case near κ_c where we apply C-periodic boundary conditions in all directions. This eliminates the complex ordered phases d_2 and d_3, with spin expectation values $\langle\phi\rangle \propto (-1 \pm i\sqrt{3})/2$, making it much easier to identify domains. However, as we only have one ordered phase left, complete wetting cannot occur.

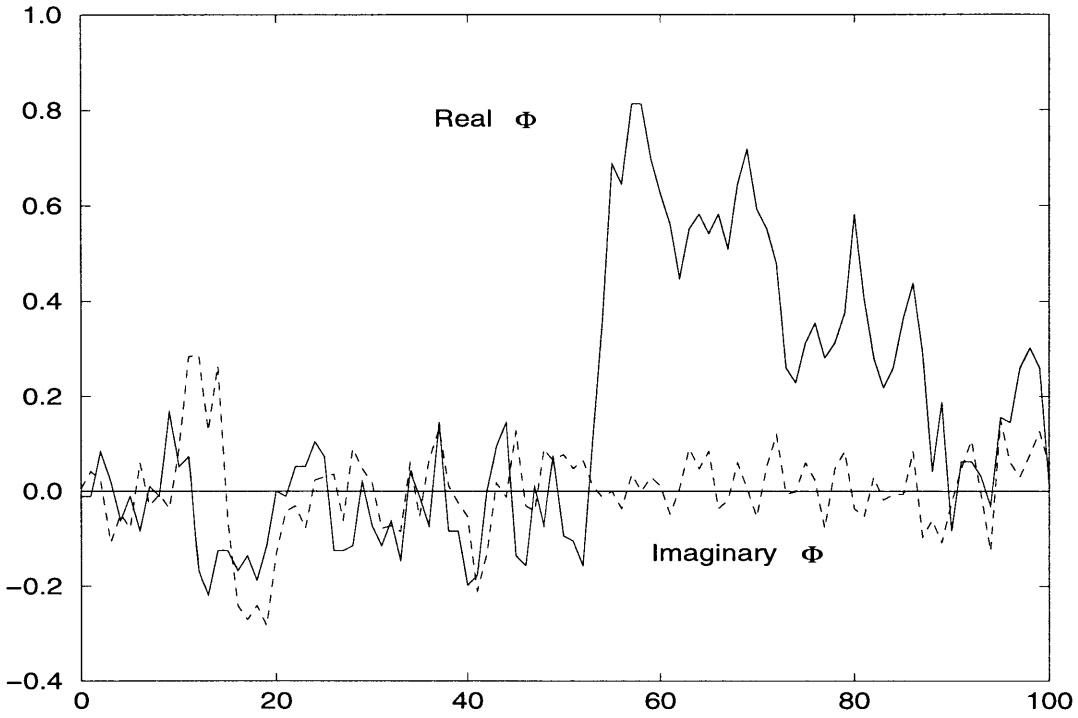

Figure 4-4: *A typical configuration near criticality where all spatial directions are C-periodic. The plot is of the real and imaginary parts of the planar average at z of the spins Φ_x versus z. There are two ordered-disordered domain walls separating ordered and disordered bulk phases.*

Using the single cluster algorithm, the numerical signal, i.e. P_{wrap}, is much larger. Because the short directions of the cylinder are also C-periodic, it is much easier to build a wrapping cluster. Unfortunately, a wrapping cluster cannot be flipped to a new state and the configuration is unchanged after this iteration. The more often we build a wrapping cluster, the longer it takes for configurations to become independent of one another. Thus, a larger signal also means larger autocorrelations. In this case, the single cluster algorithm gives much larger integrated autocorrelation times than with C-periodicity in the long direction only. This makes the algorithm terribly inefficient and, unable to generate enough statistically independent configurations, we cannot detect finite volume dependence in $\langle\Phi\rangle$.

This problem of increased autocorrelations can be solved using the multicluster algorithm. Each configuration contains many clusters and, even though the wrapping ones cannot be flipped, there are always many non-wrapping ones which can be. This generates independent decorrelated configurations quite quickly and we are able to

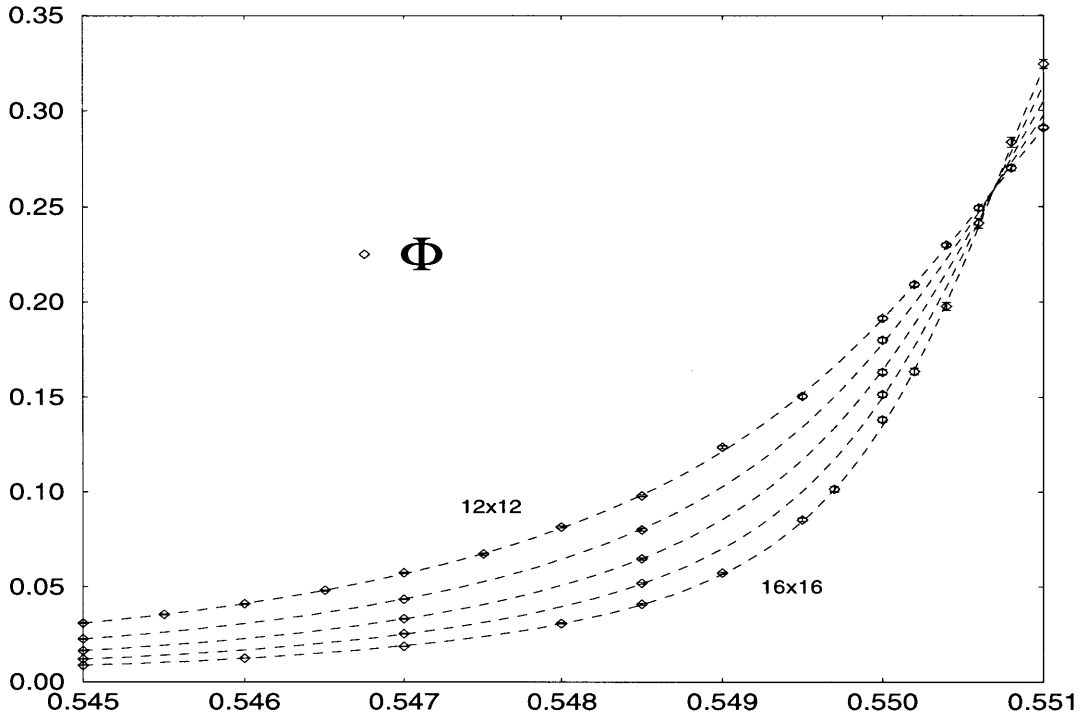

Figure 4-5: *A plot of* $\langle\Phi\rangle$ *versus* κ *in cylinders of length* $L_z = 80$ *and areas from* 12×12 *to* 16×16. *The curves are the fit to the predicted analytical behavior of* $\langle\Phi\rangle$ *across the phase transition.*

reliably estimate the average spin. Using this algorithm, we examine cylinders with dimensions $L_x = L_y = 12, 13, 14, 15, 16$ and $L_z = 60, 70, 80, 90$ and at couplings in the range $\kappa \in [0.545, 0.551]$. Again, a typical simulation has 10 000 iterations to thermalize the system and 1 000 000 to perform measurements. In Figure 4-4, we plot a typical configuration in a cylinder of dimension $12 \times 12 \times 100$ at $\kappa = 0.549$, again using the planar averages of the spins to determine the domains. This configuration has two domains of disordered phase where Φ fluctuates around 0 and one ordered domain where Φ fluctuates around Φ_0. There are two ordered-disordered domain walls in this configuration.

The multicluster algorithm decomposes the entire volume into clusters in every iteration. The integrated autocorrelation times are quite small and we measure the average spin in each simulation with a statistical error of about 1%. We fit all of the numerical data to the predicted analytical behavior of $\langle\Phi\rangle$.

In Figure 4-5, we plot some of the numerical data and the fit of $\langle\Phi\rangle$ as a function

of κ. From the fit of all the data, we find the ordered-disordered interface tension is $\alpha_{cd} = 0.0015(2)$, with $\chi^2/\text{d.o.f} \sim 1.1$, which we take as a reasonable fit. Translated into our notation, a value of $\alpha_{cd} = 0.00148(2)$ has previously been found [8], with which our value is consistent. From the fit, we also obtain $\kappa_c = 0.55070(17)$, in comparison to the previously quoted value $\kappa_c = 0.550565(10)$ [8], which are again consistent with one another. We feel that the relatively large percentage errors in our estimates of the interface tension and the critical coupling may be because we work in smaller volumes. Also, we require 14 parameters to fit the data to the analytic behavior over this range of κ. In such a large parameter space, it is quite difficult to determine all parameters very accurately.

Interestingly, if we extrapolate the linear fit of the ordered-ordered interface tension $\alpha_{dd}(\kappa)$ to the critical point, we find $\alpha_{dd}(\kappa_c) = 0.0068$. If complete wetting occurs at the phase transition, then $\alpha_{dd}(\kappa_c) = 2\alpha_{cd}$, which implies that $\alpha_{cd} = 0.0034$, which we see is too large by a factor of 2. This corroborates our earlier statement, that we cannot make a valid extrapolation to the critical point of the ordered-ordered interface tensions determined far from κ_c.

4.6 Summary

Analytically, we predicted that a very unusual type of confinement occurs even in the deconfined phase of $SU(3)$ Yang-Mills theory. The signal for this unusual confinement is that the expectation value of the Polyakov loop becomes exponentially small. We successfully observe this unusual confinement numerically in an effective theory for the pure gauge theory. To measure the exponentially small signal, we had to examine moderately sized volumes, where it was not a priori clear that the dilute interface gas calculation was valid. Using a highly efficient single cluster algorithm, we were able to observe the domain wall structure far from criticality even in moderate volumes. Using an improved estimator, we could measure the finite volume dependence and extract $\alpha_{dd}(\kappa)$ the interface tension of domain walls between ordered (analog of deconfined) bulk phases.

Near criticality and imposing C-periodicity in the cylinder's long direction only, the signal became too small to be reliably measured using either the single or multicluster algorithm. This meant we could not test our analytic calculation. Because of large fluctuations in the bulk phases, it was not possible to determine the domains clearly and we could not confirm that complete wetting occurs at the phase transition.

Imposing C-periodicity in all directions near criticality, we eliminate two of the ordered phases. The single cluster algorithm becomes terribly inefficient and does not produce as many statistically independent configurations as are required to detect finite volume dependence. The multicluster algorithm is far superior and efficiently produces independent configurations, where the domain wall structure is easily visible. Again using an improved estimator, we observe the predicted analytic behavior, which we use to numerically determine α_{cd} and κ_c. the ordered-disordered (confined-deconfined) interface tension and critical coupling respectively.

From our results, we see that the expansion of a dilute gas of interfaces is valid in the modestly sized volumes we have examined. The predicted analytic behavior is observed and our new technique is successfully applied to determine the energy cost of domain walls, which we have checked are consistent with previous work.

Chapter 5

Conclusions

5.1 Summary of results

In Chapter 2, we examined supersymmetric $SU(N)$ Yang-Mills theory at zero and non-zero temperature. We constructed effective models to describe domain walls in these theories. At zero temperature, we found situations where complete wetting of confined-confined domain walls occurs. The interface splits into two parallel interfaces, separated by a layer of non-Abelian Coulom phase. Each confined region has gluino condensate value $\chi^{(n)} = \chi_0 \exp(2\pi i n/N), n \in \{1, ..., N\}$. A domain wall separates regions with condensate values $\chi^{(m)}$ and $\chi^{(n)}$. For N even and $m - n = N/2$, complete wetting always occurs. For N odd or $m - n \neq N/2$, complete wetting only occurs provided that the domain walls are not BPS states. The critical exponents of the wetting are consistent with long-range interactions between domain walls, which we expect as we assume there is a massless Coulomb phase present. We also found complete wetting of domain walls at a non-zero temperature, where we assume that there is simultaneously a deconfinement and a chiral symmetry restoring phase transition. The critical behavior of the wetting is as expected from short-ranged domain wall interactions, as all phases are massive. The wetting provides a mechanism which explains how a QCD string carrying color flux can end on a domain wall, which does not carry color charge. This field theoretic explanation is much simpler than the String Theory description. The mechanism is only possible if deconfinement and

chiral symmetry restoration occur at the same temperature. This leads us to the prediction that deconfinement and chiral symmetry breaking occur at the same temperature in supersymmetric $SU(N)$ Yang-Mills theory.

In Chapter 3, we calculated analytically the free energy of a test quark in cylindrical volumes. We found that, paradoxically, the free energy diverges with the cylinder length, i.e. the quark is confined, even deep in the deconfined phase of the theory. This is due to the cylinder containing multiple deconfined domains separated by domain walls. We also calculated the finite volume dependence of the quark's free energy near the phase transition, which depends on the energy cost of the domain walls. This is evidence that the domain walls observed in the Euclidean theory correspond to physical domain walls in Minkowski space-time. It is also a new method which allows us to extract numerical parameters such as the QCD string tension σ and the energy cost per unit area of domain walls (the interface tension) α from numerical simulations.

In Chapter 4, we examined numerically an effective lattice model for $SU(3)$ pure gauge theory. Using highly efficient cluster algorithms, we were able to detect the analog in this model for confinement in the deconfined phase. From the finite volume dependence, we could also sucessfully apply our new method to determine the interface tensions of domain walls far from and close to criticality.

5.2 Comparison of previous and present work

Our investigation of the supersymmetric gauge theory was prompted by a claim made using Matrix-theory methods in String Theory. The phenomenon of a QCD string ending on a domain wall has been previously discussed in this framework. Ours is the first field theoretic explanation of how this phenomenon occurs. We also explain how it is necessary for the domain walls to be of infinite extent and to be completely wet for the QCD string to end on the wall. Ours is the first field thoeretic method that we know of which predicts simultaneous deconfinement and chiral symmetry restoration in the supersymmetric gauge theory.

The dilute interface gas expansion has been used previously to extract the energy spectrum from correlation functions. We are the first to use it to predict the unusual confinement in the deconfinement phase. The finite volume dependence of the quark energy has not previously been calculated. This technique has previously been used to determine interface tensions, but not with the same accuracy.

There has been previous work using twisted or dynamical boundary conditions in numerical simulations to force domain walls into typical configurations [51]. In our simulations, domain walls appear quite naturally. Much work has previously been done on measuring interface tensions and the critical temperature using many techniques [8]. The values we determine are consistent with these.

5.3 Prospects for future work

The supersymmetric pure gauge theory is under active investigation. It has been shown that chiral symmetry breaking does indeed occur when the gauge group is $SU(2)$ [21]. There has also been work done on the phase structure of $SU(3)$ gauge theory with $N_f = 2$ flavors of adjoint massless Dirac fermions [37]. This has shown that the deconfinement and chiral symmetry breaking phase transitions occur at separate temperatures. The supersymmetric case with adjoint massless Majorana fermions corresponds to $N_f = 1/2$, which has yet to be fully examined numerically. Our claim for the phase structure remains to be confirmed or disproved. The domain walls of the theory split at the high-temperature phase transition due to complete wetting. This would correspond to the splitting of a D-brane in the String Theory. There may be some interesting investigation to be done to see what the effects of such splitting might be.

Using our finite volume formulae, we are able to extract the interface tensions α for a rather simple spin model, which is an effective model for the pure gauge theory. This shows that it is at least possible in principle to use the same method to measure the QCD string tension σ and the interface tensions in the full gauge theory. We have not yet done this. It may also be possible to use the interface gas expansion in

the supersymmetric pure gauge theory at high temperature, where both the Polyakov loop Φ and the gluino condensate χ will be volume dependent.

It is universally agreed that the domain walls which appear in numerical simulations of pure gauge theory are essential to the description of the Euclidean theory. The dependence of the quark free energy on the domain walls is evidence that these walls are physical objects in Minkowski space-time. It may be possible in the future to resolve this question.

Bibliography

[1] M. Lüscher, K. Symanzik and P. Weisz, *Nucl. Phys.* **B173** (1980) 365.

[2] H.D. Politzer, *Phys. Rev. Lett.* **30** (1973) 1346;
D.J. Gross and F. Wilczek, *Phys. Rev. Lett.* **30** (1973) 1343.

[3] A. Campos, K. Holland and U.-J. Wiese, *Phys. Rev. Lett.* **81** (1998) 2420;
A. Campos, K. Holland and U.-J. Wiese, *Phys. Lett.* **B443** (1998) 338;
A. Campos, K. Holland and U.-J. Wiese, `hep-lat/9809062`.

[4] K. Holland and U.-J. Wiese, *Phys. Lett.* **B415** (1997) 179;
K. Holland and U.-J. Wiese, *Nucl. Phys. Proc. Suppl.* **63** (1998) 448.

[5] K. Holland, `hep-lat/9902027`.

[6] A.M. Polyakov, *Phys. Lett.* **B72** (1978) 477;
L. Susskind, *Phys. Rev.* **D20** (1979) 2610.

[7] L.D. McLerran and B. Svetitsky, *Phys. Rev.* **D24** (1981) 450;
B. Svetitsky, *Phys. Rep.* **132** (1986) 1.

[8] W. Janke and R. Villanova, *Nucl. Phys.* **B 489 [FS 14]** (1997) 679, and references therein.

[9] J. Engels, J. Fingberg and M.Weber, *Nucl. Phys.* **B332** (1990) 737;
J. Engels, J. Fingberg and D.E. Miller, *Nucl. Phys.* **B387** (1992) 501.

[10] R. V. Gavai, F. Karsch and B. Petersson, *Nucl. Phys.* **B322** (1989) 738;
M. Fukugita, M. Okawa and U. Ukawa, *Phys. Rev. Lett.* **63** (1989) 1768;
N.A. Alves, B.A. Berg and S. Sanielevici, *Phys. Rev. Lett.* **64** (1990) 3107.

[11] J. Cleymans, R.V. Gavai and E. Suhonen, *Phys. Rep.* **130** (1986) 217;
L. McLerran, *Rev. Mod. Phys.* **58** (1986) 1021.

[12] J. Ignatius, K. Kajantie, H. Kurki-Suonio and M. Laine, *Phys.Rev.* **D49** (1994) 3854.

[13] S. Dietrich, *Phase Transitions and Critical Phenomena* **Volume 12**, edited by C. Domb and J.L. Lebowitz (Academic Press, London) 1988.

[14] J. Goldstone, *Nuovo Cimento* **19** (1961) 15.

[15] K. Rajagopal, *Quark-Gluon Plasma 2*, edited by R. Hwa (World Scientific) 1995.

[16] F. Karsch and E. Laermann, *Phys. Rev.* **D50** (1994) 6954;
J. Engels et al., *Phys. Lett.* **B396** (1997) 210.
F. Karsch, `hep-lat/9903031`.

[17] E. Shuryak, *Phys. Lett.* **B107** (1981) 103.

[18] S. Coleman and J. Mandula, *Phys. Rev.* **159** (1967) 1251.

[19] N. Seiberg, *Nucl. Phys.* **B435** (1995) 129.

[20] J. Bell and R. Jackiw, *Nuovo Cimento* **60A** (1969) 47;
S. Adler, *Phys. Rev.* **177** (1969) 2426.

[21] R. Kirchner, S. Luckmann, I. Montvay, K. Spanderen and J. Westphalen, *Phys. Lett.* **B446** (1999) 209.

[22] E. Witten, *Nucl. Phys.* **B507** (1997) 658.

[23] A. Kovner, M. Shifman and A.V. Smilga, *Phys. Rev.* **D56** (1997) 7978;
G. Dvali and M. Shifman, *Phys. Lett.* **B396** (1997) 64;

M. Shifman and M.B. Voloshin, *Phys. Rev.* **D57** (1998) 2590;
A.V. Smilga and A.I. Veselov, *Nucl. Phys.* **B515** (1998) 5195;
G. Dvali and Z. Kakushadze, *Nucl. Phys.* **B537** (1999) 297.

[24] K. Intriligator, N. Seiberg and S.H. Shenker, *Phys. Lett.* **B342** (1995) 152.

[25] F.R. Buff, *Handbuch der Physik* **Volume 10** (Springer, Berlin) 1960 p. 288.

[26] B. Widom, *J. Chem. Phys.* **62** (1975) 1332.

[27] F. Iglói and J.O. Indekeu, *Phys. Rev.* **B41** (1990) 6836;
C. Ebner, F. Hayot and J. Cay, *Phys. Rev.* **B42** (1990) 8187.

[28] K. Binder, *Acta Polymer* **46** (1995) 204.

[29] R. Leidl, A. Drewitz and H.W. Diehl, `cond-mat/9704215`.

[30] J.O. Indekeu and J.M.J. van Leeuwen, *Phys. Rev. Lett.* **75** (1995) 1618.

[31] J. Bischof, D. Scherer, S. Herminghaus and P. Leiderer, *Phys. Rev. Lett.* **77** (1996) 1536.

[32] R. Lipowsky, *Phys. Rev. Lett.* **52** (1984) 1429.

[33] Z. Frei and A. Patkós, *Phys. Lett.* **B229** (1989) 102.

[34] T. Trappenberg and U.-J. Wiese, *Nucl. Phys.* **B372** (1992) 703.

[35] G. Veneziano and S. Yankielowicz, *Phys. Lett.* **B113** (1982) 231;
T. Taylor, G. Veneziano and S. Yankielowicz, *Nucl. Phys.* **B218** (1983) 493.

[36] U. Ascher, J. Christiansen and R.D. Russell, *ACM Transactions on Mathematical Software* **Volume 7 No. 2** (June 1981) 209.

[37] F. Karsch and M. Lütgemeier, `hep-lat/9812023`.

[38] T.W.B. Kibble, *J. Phys.* **A9** (1976) 1387.

[39] A.V. Smilga, *Ann. Phys.* **234** (1994) 1;
T.H. Hansson, H.B. Nielsen and I. Zahed, *Nucl. Phys.* **B451** (1995) 162;
J. Kiskis, `hep-lat/9510029`.

[40] E. Hilf and L. Polley, *Phys. Lett.* **B131** (1983) 412.

[41] A.S. Kronfeld and U.-J. Wiese, *Nucl. Phys.* **B357** (1991) 521.

[42] U.-J. Wiese, *Nucl. Phys.* **B375** (1992) 45.

[43] B. Grossmann, M.L. Laursen, T. Trappenberg and U.-J. Wiese, *Nucl. Phys.* **B396** (1993) 584.

[44] E. Brezin and J. Zinn-Justin, *Nucl. Phys.* **B257 [FS14]** (1985) 867;
V. Privman and M.E. Fisher, *J. Stat. Phys.* **33** (1983) 385.

[45] K. Kajantie, L. Kärkkäinen and K. Rummukainen, *Nucl. Phys.* **B333** (1990) 100; *Nucl. Phys.* **B357** (1991) 693.

[46] M. Creutz, *Quarks, Gluons and Lattices* (Cambridge University Press, 1983).

[47] N. Metropolis, A.W. Rosenbluth, M.N. Rosenbluth, A.H. Teller and E. Teller, *J. Chem. Phys.* **21** (1953) 1087.

[48] F. Niedermayer, `hep-lat/9704009`.

[49] R.H. Swendsen and J.S. Wang, *Phys. Rev. Lett.* **58** (1987) 86;
U. Wolff, *Phys. Lett.* **B228** (1989) 379.

[50] M. Caselle, F. Gliozzi, P. Provero and S. Vinti, *Nucl. Phys. Proc. Suppl.* **34** (1994) 720.

[51] M. Caselle and M. Hasenbusch, *Nucl. Phys.* **B470** (1996) 435.